PENNSTATE

Applied Research Laboratory

Annual Report
1 Feb 1992 to 31 Jan 1993

STUDIES OF SEVERAL SMALL SEAWATER MHD THRUSTERS USING THE HIGH-FIELD SOLENOID OF MIT'S BITTER MAGNET LABORATORY

Sponsored By

Department of the Navy
Office of Naval Research
Grant No. N00014-89-J-1693

Prepared By

T. F. Lin, D. L. Aumiller, J. B. Gilbert, and M. J. Coslo
February 1993

Applied Research Laboratory
The Pennsylvania State University
P.O. Box 30
State College, PA 16804

ABSTRACT

The performance of several small, seawater magnetohydrodynamic (MHD) thrusters was studied in a closed loop environment. Three different thrusters were designed, constructed, and evaluated. For the first time, videographic and photographic recordings of flow through an MHD thrusters were obtained. The MHD induced flowrate, thrust, and mechanical efficiency was measured/calculated for each thruster at different combinations of electric current and magnetic field strength. Direct determination of thrust, and subsequently of efficiency were not possible. Therefore, the hydraulic resistance of each different thruster was correlated with flowrate. This information was used in conjunction with the measured MHD induced flowrate to calculate the thrust and efficiency of each thruster. Experimental results were repeatable. A theoretical model was developed to predict the performance of each thruster. The results of this model are presented for one thruster at several magnetic field strengths at various electric currents. These predictions corresponded well with the measured/calculated values of MHD induced flowrate and mechanical efficiency. Finally, several MHD thrusters with radically different configurations are proposed.

TABLE OF CONTENTS

TABLE OF CONTENTS (Continued)

TABLE OF CONTENTS (Continued)

LIST OF FIGURES

LIST OF FIGURES (Continued)

NOMENCLATURE

A	cross-sectional area (m^2).
B	magnetic field strength (*Tesla*).
D	distance between the electrodes (m).
D_h	hydraulic diameter (m).
f	friction factor.
G	mass flux ($kg/m^2 \cdot s$).
g_c	gravitational constant (m/s^2).
I	current across the electrodes (A).
L	length of the MHD thruster (m).
Δp_a	two-phase acceleration pressure drop (*psi*).
$\Delta p_{1\phi}$	single-phase pressure drop (*psi*).
$\Delta p_{2\phi}$	two-phase pressure drop (*psi*).
R	electrical resistance (Ω).
Re	Reynolds number.
R_f	two-phase friction multiplier.
T	thrust (N).
U	fluid velocity (m/s).
V	voltage potential between electrodes (*volt*).
V_o	overpotential (*volt*).
v_f	specific volume of the fluid (m^3/kg).
v_g	specific volume of the gas mixture (m^3/kg).

α_e	void fraction at channel exit.
χ_e	exit quality.
η	fraction of Cl_2 that does not dissolve into seawater.
η_m	mechanical efficiency (%).
ρ	density of seawater (kg/m^3).
σ	specific conductivity (Ω/m).

ACKNOWLEDGEMENTS

This work was supported principally by the Office of Naval Research Grant No. N00014-89-J-1693 with Dr. Gabriel D. Roy as Scientific Officer, and in part by the Applied Research Laboratory of The Pennsylvania State University.

We wish to also thank Tom Imblum, Joe Naggar, Rich Johnson and Rick Hans their technical support in operation and maintenance of the loop.

We would like to thank Larry Rubin and the rest of the staff at the Francis Bitter National Magnet Laboratory. Without their help and knowledge these studies would have been impossible.

The National Science Foundation is also acknowledged for their funding of the National Magnet Laboratory.

Chapter 1

Introduction

1.1 Objective

The purpose of this study was to design, construct and analyze several small seawater magnetohydrodynamic (MHD) thrusters. A predictive, analytical model was used to aid in the design of two generations of MHD thrusters. A technique of quantitatively evaluating the performance of the thrusters was developed. Using this procedure all of the test sections were extensively studied to determine their operating characteristics. The parameters used to examine the performance are: the volumetric flowrate induced by the thruster, the thrust generated and the mechanical efficiency of the test section.

1.2 Basic Concepts of MHD Propulsion

The presence of salts allows seawater to conduct electricity by electrolytic ion exchange. Thus by passing an electric current through seawater in the presence of a magnetic field, a Lorentz (**j x B**) force will act to move the seawater in the direction normal to both the magnetic field and electric current directions. This allows for a non-intrusive method of pumping water. This is an advantage because it removes the acoustic signature of the propeller which makes detection of the MHD driven vehicle much more difficult. An additional benefit is that MHD propulsion, unlike a propeller, does not have a cavitation limiting maximum velocity.

The basic idea of MHD propulsion has existed since 1962. However, the most

inhibiting factor has always been the availability of magnets with high enough magnetic fields. This problem has in part been solved by the advent of superconducting magnets. The superconducting magnets are only charged with current once, whereas electromagnets need a continual source of large d.c currents, typically tens of kiloamps.

A prototype ship utilizing MHD has recently been constructed in Japan. The YAMATO-1, sponsored by Japan's Ship & Ocean Foundation, uses two thrusters manufactured by Mitsubishi and Toshiba Heavy Industries. Each thruster is capable of 4,000 *N* of propulsive thrust. The ship is approximately 30 meters in length and displaces roughly 185 tons. The YAMATO-1 is designed to reach a speed of 8 knots. To date, there has been limited testing of this vessel [1,2].

1.3 Previous Work Performed at Penn State

In 1988 the Applied Research Laboratory at the Pennsylvania State University began research in the field of MHD propulsion. This study utilized a "dual control volume" technique to determine vehicle speed as a function of thruster configuration. The results were quite encouraging [3]. It was predicted that an MHD thruster could obtain comparable performance characteristics as a screw propeller.

In an attempt to increase the efficiency of MHD thrusters, conductivity enhancement experiments were conducted. The effects of the addition of acids to the seawater was studied. Both uniform mixing and pulse injection methods were conducted and analyzed. Both methods were shown to substantially increase the conductivity of the seawater. It was concluded that the pulse injection method more closely represented the

manner in which a functioning MHD thruster would perform conductivity enhancement, and was studied in more detail [4].

The electrolysis of seawater is an integral part of MHD propulsion and as such several aspects of this process have been studied at Penn State. Experiments and analysis performed by Naggar et.al. [5] examined the phenomenon of overpotential for several cathode materials. The effect of changing fluid velocity was studied.

Another phenomenon associated with the electrolysis of seawater is the production of electrolytic gases. When the electrolytic ions reach the oppositely charged electrode, gaseous microbubbles are formed. This has several implications for MHD propulsion. The first is that the gases are nonconductive and will decrease the effective conductivity of the seawater. Additionally, the bubbles increase the frictional losses in the thruster due to the two-phase effect. The bubbles also could create a means of optical or acoustic detection, which could offset the stealth advantages of MHD propulsion. Chlorine gas is produced at the anode. However chlorine is slightly soluble in seawater. Therefore knowledge concerning the amount of chlorine gas that escapes the thruster is important. This problem was addressed by Marks [6] and Imblum [7]. The two studies were identical except in the manner in which the specific volume of the "equivalent gas" was calculated. From these studies it was determined that between 25 and 60% of the chlorine initially produced escapes a typical test section.

Following these in depth studies the next logical step was the design and construction of an operating MHD thruster.

1.4 Overview of Closed Loop MHD Experiments

All of the MHD experiments detailed in this study were conducted at the Francis Bitter National Magnet Laboratory, at the Massachusetts Institute of Technology (MIT). A solenoid magnet with a peak magnetic field of 8 *Tesla*, directed vertically upward, was utilized. The magnet had an available bore diameter of 9¾-*in*, and used 40,000 *amps* to achieve its maximum field. There are several advantages and disadvantages this magnet. Due to the magnet's solenoid design there was an optical path to the warm bore. This was used for the photographic and videographic recordings of the two-phase MHD-induced flows. This optical access does not exist for dipole magnets. Its relatively small warm bore, compared to a dipole, sharply curtails the performance of an MHD thruster. Additionally, the magnetic field strength could be varied as a function of time which can provide a very good relationship between the magnetic field strength and performance of a thruster. The ability to ramp the magnetic field usually does not exist for superconducting magnets.

The test sections were constructed of an optically clear material which housed two electrodes. The electrodes were oriented such that the current flow was normal to the magnetic field, which produced the maximum Lorentz force. The test section was connected to a 40 gallon tank. The plumbing from the tank to the test section included a flowmeter capable of measuring the MHD-induced flow. Once the two-phase mixture returns to the tank, the gases were vented out of the test loop.

Chapter 2

Analytical Approach

2.1 Overview

Before an MHD thruster could be constructed, several analytical tools were developed. The first tool was an analytical model which would aid in the design of the test section. Using this model the geometry of the test section could be varied to optimize performance. The second tool was a methodology which allowed the test section's thrust and efficiency to be inferred from knowledge of the MHD-induced flow rate.

2.2 Predictive Analytical Model

The methodology of the model which has been developed to predict flow rate as a function of voltage and magnetic field strength equates the pressure drop around the specific test loop and the pressure rise which the thruster creates. According to the Lorentz Law, the force created by the thruster is

$$\vec{F} = \vec{J} \times \vec{B} \tag{2.1}$$

where

$\vec{F}$ = *the resultant Lorentz Force vector*

$\vec{J}$ = *the electric current density vector*

and $\vec{B}$ = *the magnetic field vector.*

If the current is everywhere normal to the magnetic field then Equation (1) simplifies to

$$F = IBD \tag{2.2}$$

where

I = *the electric current through the thruster*

B = *the magnetic field strength*

and D = *the distance between the electrodes*

Using this definition, pressure rise due to the Lorentz force is,

$$\Delta p_{rise} = \frac{IDB}{A_{flow}} \qquad (2.3)$$

where

A_{flow} = *the thruster's flow area.*

where the flow area is the cross-sectional area of the thruster through which the water flows.

2.2.1 Relationship Between Voltage and Current

In order to use Equation (2.3), the relationship between the current, magnetic field, fluid velocity in the test section (U) and overpotential (the minimum voltage required for electrolysis) must be ascertained. There are two phenomena which diminish the electric potential: the back electromotive force (EMF) and overpotential. The back EMF is a voltage that is induced by the motion of an electrical conductor in a magnetic field. The magnitude of this voltage is,

$$V_B = BUD. \qquad (2.4)$$

The current thruster design utilizes Hastelloy-C as the cathode, and the anode is a titanium coated with a rare-earth oxide. This is marketed under the trade name of DSA (Dimensionally Stable Anode). For this electrode combination the overpotential, V_o, is approximately 2.25 volts. Therefore the current can be calculated from,

$$I = \frac{V - V_o - BUD}{R}. \tag{2.5}$$

To calculate the resistance of the test section the following equation was employed

$$R = \frac{D}{A_{ele}\,\sigma_{effective}} \tag{2.6}$$

where

A_{ele} = *average current passage area*

and $\sigma_{effective}$ = *effective specific conductivity of the seawater.*

The specific conductance of water at between 4-5 *mho/m*. A value of 5 *mho/m* was used throughout the analysis. The effective specific conductivity decreases with increasing void fraction that comes from electrolysis.

2.2.2 Calculation of Pressure Drop

The above equations can be used to calculate the pressure rise in the thruster, which in the steady state is countered by the frictional and form pressure losses around the test loop. The next step is to predict the magnitude of these losses for a given flowrate.

To ease the calculation of the pressure drops, the loop can be divided into two parts, a single phase region and a two phase region. The single phase region extends from the outlet of the tank to the entrance of the test section. The two phase region is from the entrance of the test section to the inlet of the tank. It should be noted that for the purposes of pressure drop calculations the tank was modeled as an infinite reservoir. Also since the loop is modeled as a whole, all gravitational terms will be omitted. This is because the elevation head lost in one part of the loop is gained in another.

There were different trips made to MIT, to perform experiments with three different test sections. For illustrative purposes, the test loop dimensions from the April, 1992 experiments with the second variation of the circular test section will be used. For this test loop configuration, the single phase portion of PVC is $\approx$ 97 inches long with 2 ball valves and has flow through both the run of a Tee and through the branch of a Tee. The single phase length of tygon is $\approx$ 24 inches in length. The single phase portion of acrylic is assumed to be 10 inches in length with an elbow at its entrance. The test section is allowed to be of variable dimensions, such that parametric studies can be carried out. The upcomer is 10 inches in length, and the two phase portion of tygon is 33 inches long. Since this tubing makes a bend, an elbow is also assigned to this region. Finally the PVC pipe downstream of the test section is 53 inches long with a single ball valve.

In each region, there are both frictional losses and form losses. In order to model the form losses an equivalent length was determined for the 90° elbows, T's and ball valves. The values were taken from the Crane Handbook [8] and are,

L/D = 30 (for 90° elbows)
L/D = 60 (for flow through the branch of a Tee)
L/D = 20 (for flow through the run of a Tee)
L/D = 3 (for fully opened ball valve).

For the expansion and contraction losses the following was used,

$$\Delta p = K \rho \frac{U'^2}{2} \tag{2.7}$$

where

K = *a geometric constant*

ρ = *fluid density*

and U' = *the velocity in the smaller area.*

The K-factors are different for expansion and contraction and are given by

$$K_{exp} = (1-\beta)^2 \tag{2.8}$$

and

$$K_{con} = \frac{1}{2}(1-\beta^2) \tag{2.9}$$

where

β = *the ratio of the smaller area to the larger one,*

respectively. The tank was modelled as an infinite reservoir. Therefore, the above equations were used with ß equal to zero.

The frictional losses were handled using the standard method of calculating a friction factor, f, and using

$$\Delta p_{friction} = f \frac{L}{D_h} \rho \frac{U^2}{2} \tag{2.10}$$

where

D_h = *the hydraulic diameter of the pipe.*

One of three different correlations were used to calculate the Darcy-Weisbach friction factor, f, depending on the Reynold's Number. The three correlations are [9]

$$f = \frac{64}{Re} \quad for \ Re < 2300 \tag{2.11}$$

$$f = 0.316 Re^{-0.25} \quad for \ 2300 < Re < 2 \times 10^4 \tag{2.12}$$

$$f = 0.184 Re^{-.2} \quad for \ Re > 2 \times 10^4 \tag{2.13}$$

2.2.3 Two Phase Effects

The pressure drop in the two phase region is only slightly more difficult to calculate. There is the addition of an acceleration pressure drop and the friction pressure drop is more for a two phase mixture than for single phase flow.

For any current a mass production rate of both H_2 and Cl_2 can be inferred, as the production rates are linearly proportional to the current. It can be shown that the constants of proportionality are 3.6809E-7 kg/Coulomb and 1.0464E-8 kg/Coulomb for chlorine and hydrogen respectively. It has been observed that some of the chlorine redissolves into the water. Therefore, only the fraction of chlorine that remains undissolved, η, contributes to the two phase phenomena. Determination of η in this test section would be quite cumbersome. Therefore, a value that was obtained in a similar system will be used [6]. Since chlorine will continually be redissolved into the water the two phase region will be split into four regions: the test section, acrylic, tygon, and PVC, with each region using a different value for η.

From the knowledge of the amount of gas present at any location, the mass quality can be calculated using the following relationship

$$\chi_i = \frac{\left(1.0464\times10^{-8}\frac{kg}{Coulomb}\right)I \cdot \eta_i\left(3.60809\times10^{-7}\frac{kg}{Coulomb}\right)I}{\dot{m}_{total}} \qquad (2.14)$$

where i corresponds to a given region.

If a two-phase model is assumed, once the quality is known the void fraction, α, can be determined. There are several different models that could be used. For the purposes of this study the homogeneous flow model was valid. Using this assumption the void

fraction is given by

$$\alpha_i = \frac{1}{1 + \left(\frac{1-\chi_i}{\chi_i}\right)\left(\frac{v_f}{v_g}\right)} \qquad (2.15)$$

where
v_f = *the specific volume of the fluid*
and v_g = *the specific volume of the gas.*

Since the quality equation has two components, an average value of the specific volumes of H_2 and Cl_2 was used for v_g.

Once the void fraction has been determined, the values of the two phase fiction multiplier, R_f, and the two phase acceleration pressure drop, Δp_a, can be determined. Therefore, the total pressure drop in a two phase region can be calculated using the following expression:

$$\Delta p_{2\phi} = R_f \Delta p_{1\phi} + \Delta p_a \qquad (2.16)$$

where
R_f = *the two phase friction multiplier*
$\Delta p_{1\phi}$ = *liquid only frictional pressure drop*
and Δp_a = *the acceration pressure drop.*

The Lottes-Finn correlation is used to calculate the two phase friction multiplier as a function of void fraction. It states,

$$R_f = \frac{1}{3}\left[1 + \left(\frac{1}{1-\alpha}\right) + \left(\frac{1}{1-\alpha}\right)^2\right] \qquad (2.17)$$

The acceleration pressure drop is only present in the test section because this is the only portion of the loop in which the bubbles are produced. The magnitude of this quantity

is given by

$$\Delta p_a = \frac{G^2}{g_c}\left[\left(\frac{(1-\chi)^2}{1-\alpha} - 1\right)v_f + \left(\frac{\chi^2}{\alpha}\right)v_g\right] \qquad (2.18)$$

where

G = *the mass flux.*

No two phase effects were considered for the form losses.

The presence of the non-conductive gasses will increase the electrical resistance of the test section. The effect was considered by using an effective specific conductance which is given by

$$\sigma_{effective} = \sigma_{seawater}(1 - \alpha) \; . \qquad (2.19)$$

2.2.4 Solution Technique

An iterative process is used to calculate the correct mass flow rate, for a given voltage. The model has as inputs the magnetic field strength and the voltage across the test section. The first step is to make a reasonable guess of the fluid velocity in the thruster. From this the current, thruster pressure rise and loop pressure drop can be determined. Since the Δp_{loop} is approximately proportional to the flowrate squared, if the pressure drop around the loop is smaller than the pressure rise in the thruster, a larger mass flowrate is used in the next iteration. If the thruster pressure rise is smaller in magnitude, a lower mass flowrate is used as the next guess. This process continues until the following criterion is met:

$$\frac{|\Delta p_{rise} - \Delta p_{loop}|}{\Delta p_{rise}} \leq 0.001 \qquad (2.20)$$

A computer listing of this code written in Turbo Pascal appears in Appendix A.

2.2.5 Results

The code described above was used to help determine the geometry of the test section. Once the design was decided upon it was again used to predict the performance of the thruster at different electric currents and magnetic field strengths. Figure 2.1 and 2.2 show these effects on flowrate and efficiency for the second variation of the circular test section. It should be noted that the convergence method used became numerically unstable at very small currents. Therefore the minimum current examined is approximately 4 *amp*.

2.3 Determination of Thrust and Efficiency

A direct measurement of the thrust generated by the test section is not attainable because the pressure transducer will not function properly in the presence of a magnetic field. Therefore, an indirect measurement must be made. This procedure involves determining the relationship between hydraulic resistance and volumetric flowrate. This is done by measuring the pressure rise required by a centrifugal pump to achieve a given flowrate. The results of this experiment are then fitted by an empirical correlation. Using this correlation the pressure rise generated by the thruster can be calculated from knowledge of the MHD induced flowrate. This pressure increase is multiplied by the

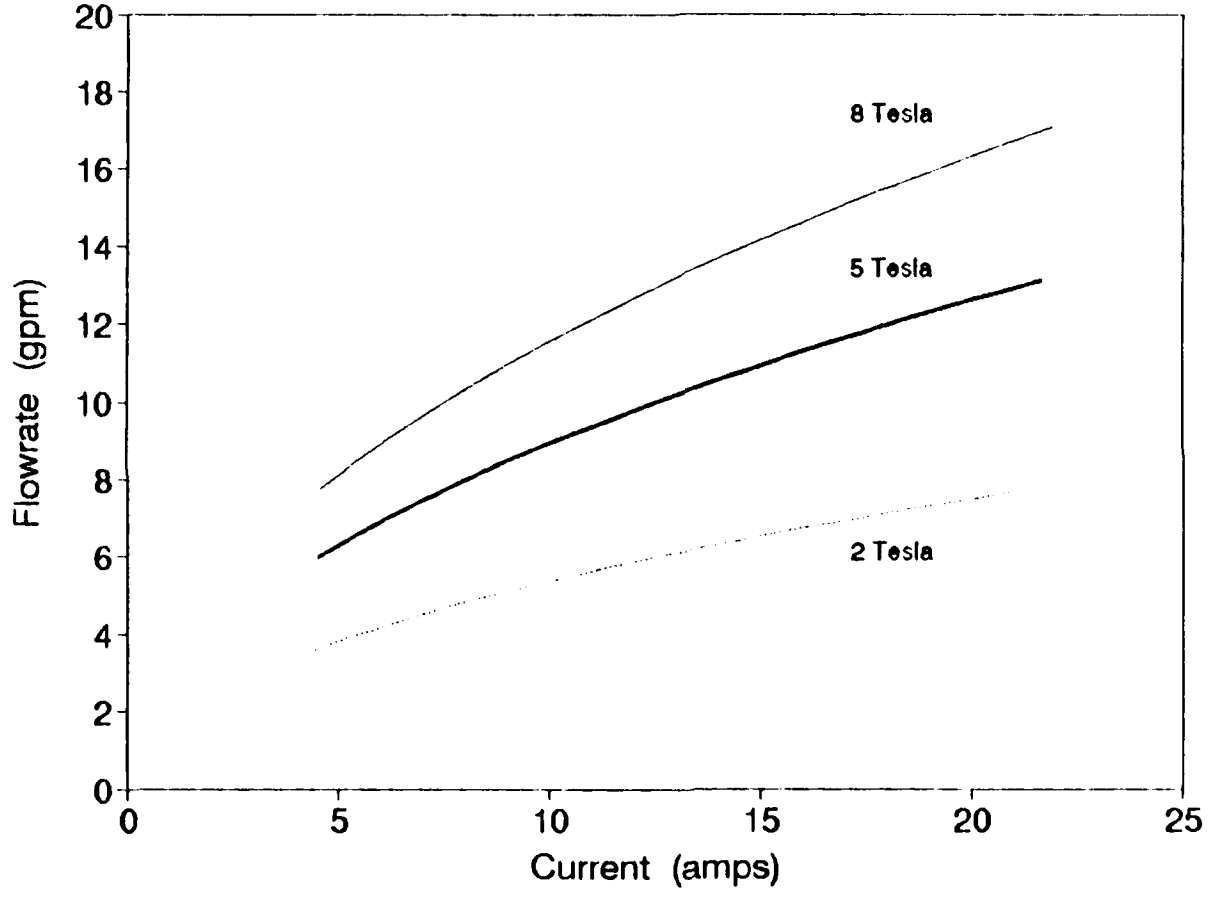

Figure 2.1 - Effect of Electric Current and Magnetic Field on the MHD Induced Flowrate for the Second Variation of the Circular Test Section

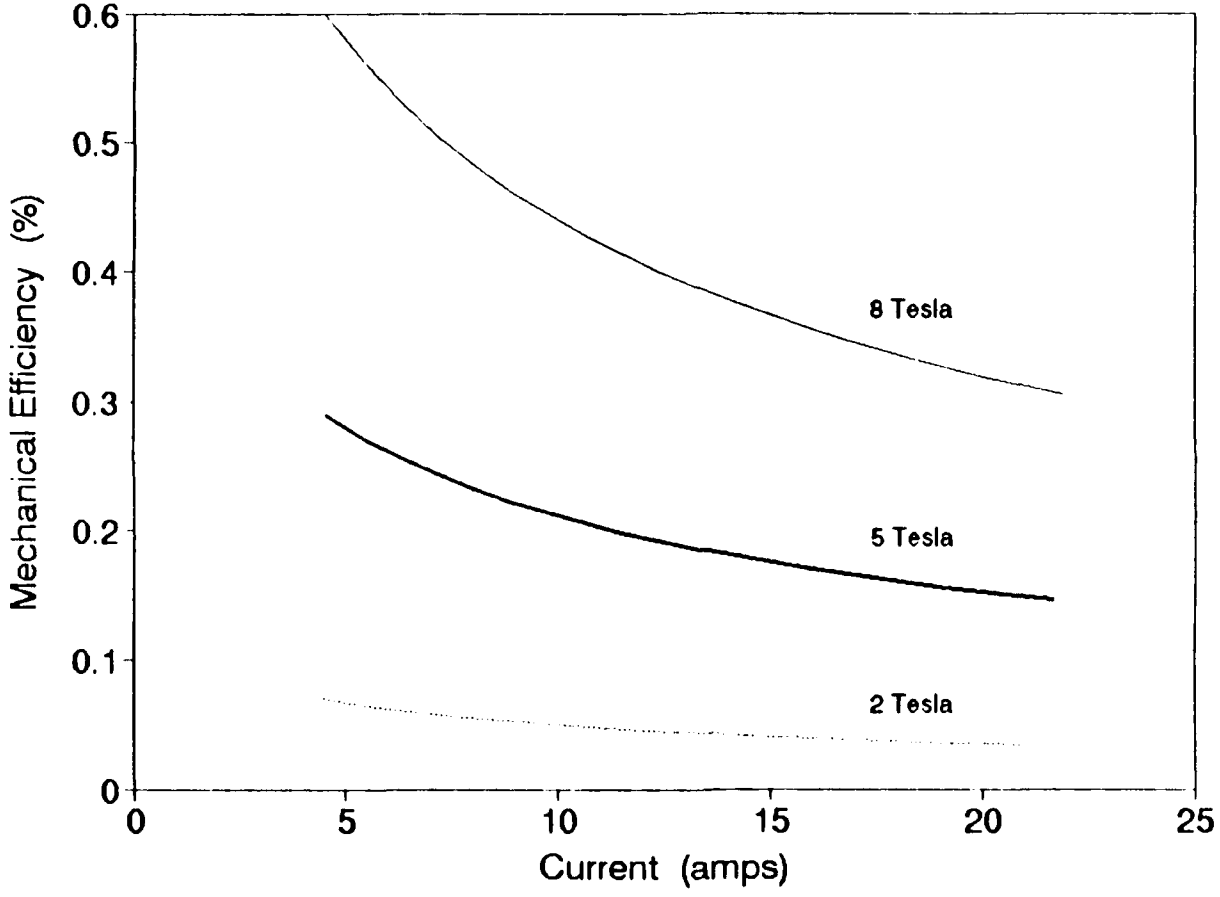

Figure 2.2 - Effects of Electric Current and Magnetic Field on the Mechanical Efficiency for the Second Variation of the Circular Test Section

thruster's flow area to determine the thrust generated. Once this is determined, the mechanical efficiency can be calculated from,

$$\eta_m = \frac{TU}{VI} \tag{2.21}$$

where
T = *thrust*
and U = *the fluid velocity in the test section.*

The velocity used in Equation 2.21 is calculated assuming that there is no gas present in the test section. This assumption provides a conservative estimation of the efficiency. The actual fluid velocity in the test section would be slightly larger because the gases occupy some of the flow area. This conservative estimation is used because there was no capability to measure the void fraction.

Chapter 3

Experimental Apparatus

3.1 MHD Driven Test Loop

The test loop utilized in performing the MHD induced flow experiments, consists of a 40 gallon reservoir, a flowmeter, an MHD thruster, 2-*in* Polyvinyl Chloride (PVC) plumbing lines, flexible tygon tubing and an auxiliary pump. Figure 3.1 is a photograph of the experimental test loop.

The auxiliary pump is configured such that it can easily be removed from the loop. Additionally the pump plumbing contains a filter canister. Two different types of filters were used. A 50 μm particle filter is used to prevent salt crystals from passing through the loop. A carbon activated filter is employed to remove some of the electrolytic contaminants. The pump can also be used, before a given run, to flush any residual bubbles from the test section for better visualization. However, at no time while an MHD induced flow experiment was underway was the auxiliary pump running.

A synthetic seawater solution is used as the electrolyte. The solution is made with filtered water and "Sea-Salt" additive. "Sea-Salt", manufactured by Lake Products Company, was chosen because it meets ASTM standards for the duplication of seawater.

3.1.1 Test Section Description

Two test section concepts were designed, manufactured and tested. The first test

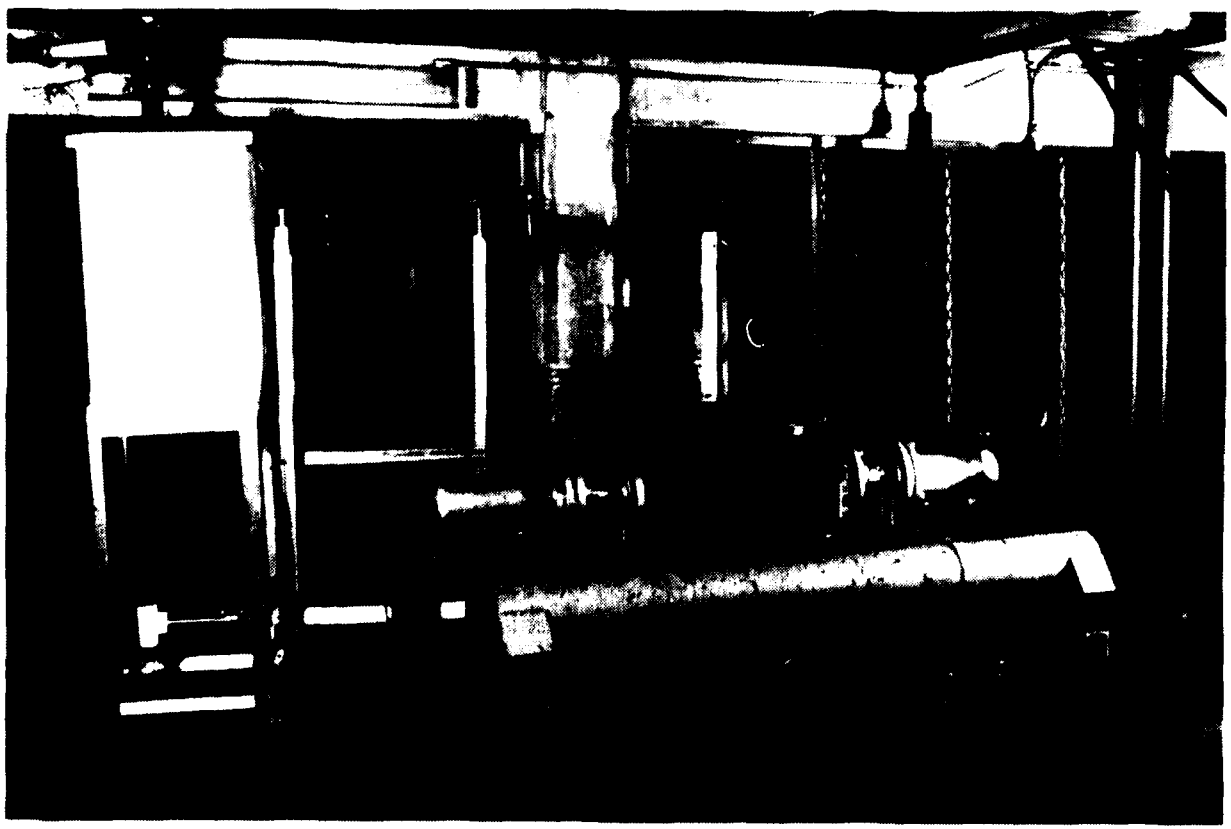

Figure 3.1 - MHD Driven Test Loop

section to be examined, designated as the circular test section, consists of a pair of 1-*in* wide and 5-*in* long electrodes placed in a pipe with a 2-*in* inner diameter. Hastelloy-C, the cathode, and Dimensionally Stable Anode (DSA) are arranged parallel to each other, and perpendicular to the magnetic field. The spacing between the electrodes is 1.732 inches. The electrodes are placed in a five inch long, optically clear test section. The materials for each electrode were chosen due to their superior resistance to electrolytic attack as seen in previous experiments. The circular test section had two variants. The first variation utilized 2-*in* Lexan to house the electrodes (see Figure 3.2). In order to achieve better optics, the second variation consisted of a Plexiglas block with a 2-*in* hole bored along one axis (see Figure 3.3). In terms of performance, both test sections had nearly identical configuration, the only difference being the increased optics of the second circular test section, which also had a 2-*in* shorter upcomer. The first circular test section was studied in the first round of experiments performed January 21-24, 1992. The second version was used in the second visit to the FBNML-MIT, April 7-10, 1992. Both variations of the circular test section had a 1¾-*in* inner diameter optically-clear pipe upstream of the thruster and a 1-*in* inner diameter optically-clear pipe downstream of the thruster. These two pipes are oriented in a vertical fashion and are connected to the thruster by specially made 90° elbows which smoothly make a transition in diameter as they redirect the fluid. The vertically-oriented, optically-clear pipe situated directly downstream of the thruster is designated as the upcomer, and the optically-clear pipe immediately upstream of the thruster will be referred to as the downcomer.

The second thruster concept, designated the rectangular test section, consisted of

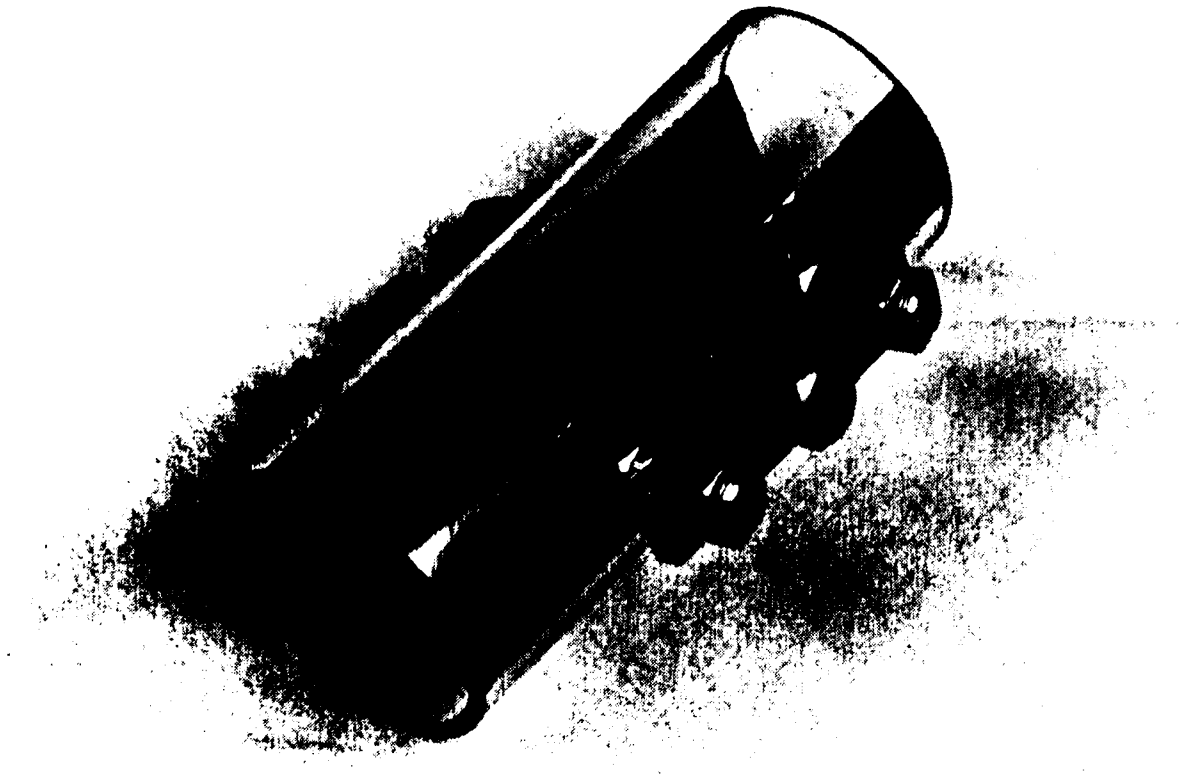

Figure 3.2 First Variation of The Circular Test Section

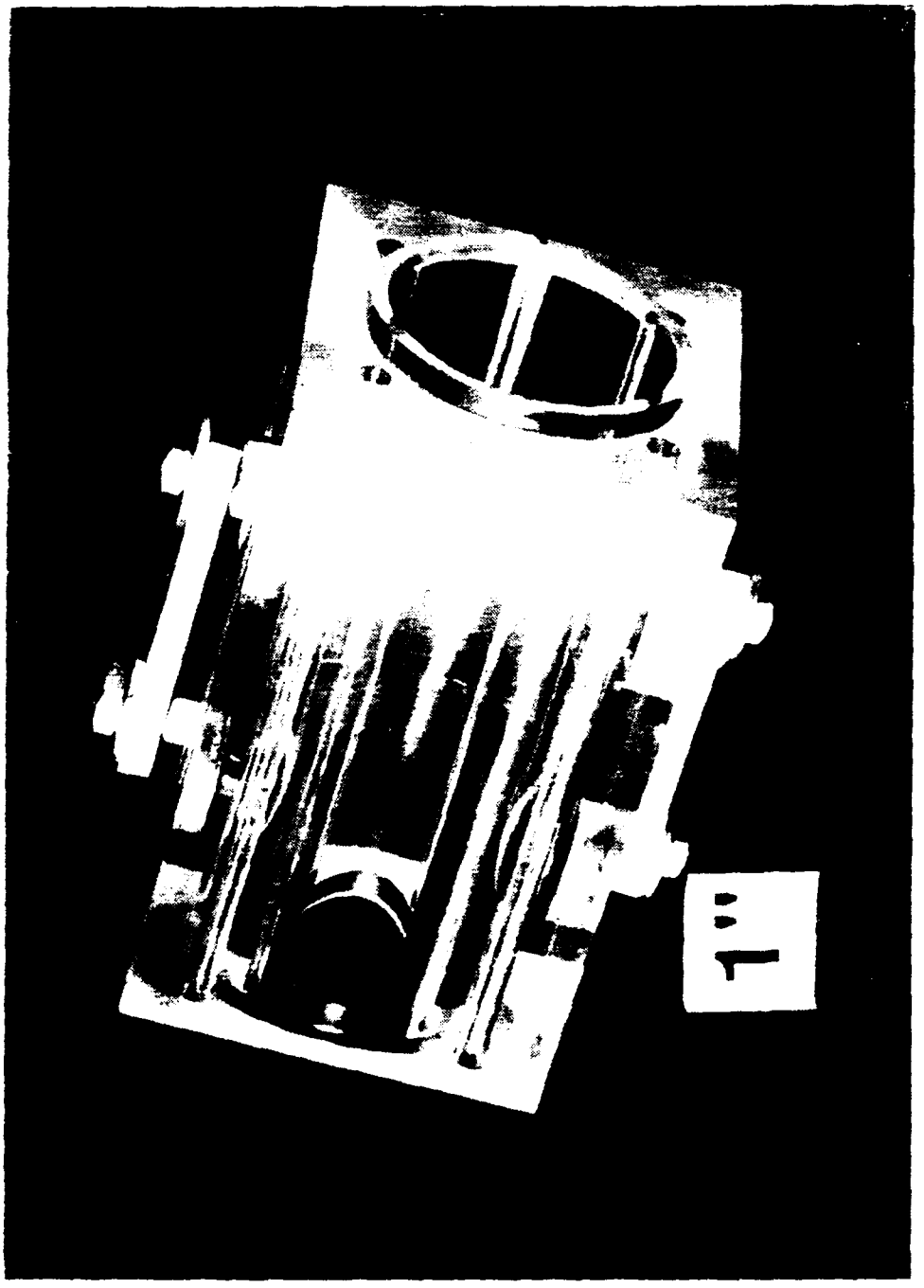

Figure 5.5 [illegible] and Variation of the [illegible]

two 5-*in* long, 6-*in* high electrodes oriented parallel to each other and normal to the magnetic field. The electrode gap for this design was chosen to be 2.125 inches. The electrode materials for this test section were the same as for the circular test sections. This test section was studied because it had a much larger hydraulic diameter than the circular test sections (3-*in* compared to 1.91-*in*). This increase in hydraulic diameter caused the rectangular test section to have a smaller frictional pressure drop than the circular ones. To further decrease the frictional pressure losses the inner diameter of the upcomer was increased to 1¾-*in*. The downcomer pipe diameter remained the same as for the circular test section.

3.1.2 Magnet

The magnet utilized in these experiments is designated as the 10-A magnet, which is owned and operated by the Francis Bitter National Magnet Laboratory (FBNML) of the Massachusetts Institute of Technology under the auspices of the National Science Foundation. The magnet is a water cooled, solenoid magnet, with the magnetic field pointing upward. The magnet requires 5000 *amps* for each tesla of magnetic field. To achieve 8 *Tesla*, the magnet must pass 40,000 *amps*. The load voltage at this condition is approximately 250 *V DC*. Therefore the magnet consumes 10 *MW* of electrical power, which needs to be removed. This is accomplished with a closed loop, heat removal system. The system uses water at 180 *psi*, with a specific resistivity of 1 $M\Omega \bullet cm$, flowing at 1,500 *gpm*. The ultimate heat sink for the magnet is the Charles River. This magnet was chosen because of its relatively large warm bore, high magnetic field,

magnetic field homogeneity, field ramping feature, and optical access to the warm bore.

3.1.3 Power Supply

An Electronic Measurements, model TCR 30 SCR, d.c. power supply was used to generate the required electric current through the test section. The power supply was able to be used as a constant voltage source or constant current source and could provide 125 *amps* at 40 *V*. Additionally, two Hewlett-Packard power supplies, capable of a combined 3 *kW*, were used. This configuration could attain higher voltages than the Electronics Measurements power supply at lower currents (50 *amps* at 60 *V*).

3.1.4 Flowmeters

In order to measure the performance of the MHD thrusters a flow measuring device was needed. Two different flowmeters were used, at different times, in these experiments. In each configuration the flowmeter was placed in the one phase region of pipe upstream of the test section.

The first flowmeter was a paddle-wheel type Data Industrial model 220-PD2 sensor coupled with a model 1000 Digital Flow monitor. This flowmeter has a range of 0 to 200 *gpm*. This flowmeter performed satisfactorily in a steady-state mode. However, due to the inertia of the large paddle wheel the flowmeter's response to a flow transient was quite slow.

An EG&G Flow Technology turbine flowmeter (Model # FT-32NEXWRLGG-5) and signal conditioner (Model # CAO3) were purchased for studying the rapidly changing

flow characteristics. This flowmeter performed better than the Data Industrial in both the steady-state and transient circumstances, and was used exclusively in the April experiments. Another subtle advantage of this flowmeter, was its decreased hydraulic resistance. One small disadvantage of this flowmeter was that it required some magnetic shielding in order to properly function. This was accomplished by using a large diameter, thick wall iron pipe placed around a thinner wall pipe made of mu-metal. This configuration allowed for acceptable magnetic field strength within this shield.

The output of both flowmeters is a square wave of varying frequency. A frequency to voltage converter is utilized to convert the output to a 0-10 *V DC* signal, which was used as an input for the data acquisition system.

3.2 Data Acquisition Systems

The nature of MHD experiments is such that several physical parameters need to be monitored simultaneously (i.e. flowrate, electrode current and voltage, etc). To accomplish this a computerized data acquisition system was employed.

There were two different systems used during the course of the experiments, one used at MIT, the other at Penn State. The inputs for both data acquisition systems required 0 to 10 *V DC* signals. To achieve this many of the outputs from the monitoring devices needed to be conditioned.

3.2.1 Data Acquisition System Used at MIT

While performing the MHD induced flow experiments, MIT's computerized data

acquisition system was used. Their system consisted of a Macintosh computer running the Labview 2.2 software package. The program was configured to simultaneously monitor eight analog (0 to 10 *V DC*) to digital channels and record the input voltage every 10 *msec*. For the steady state cases, eleven seconds worth of data were averaged per data point. The following parameters were monitored during the MHD induced flow experiments: tank temperature, ambient temperature, system flowrate, voltage across electrodes, electric current between electrodes, and magnetic field strength.

3.1.7 Data Acquisition System Used at Penn State

There were several experiments which needed to be performed at Penn State prior to making the trips to MIT. These experiments required the use of a variable speed pump and a data acquisition system. The data acquisition system used for the studies done at Penn State consisted of a Gateway 2000 Personal Computer with a high speed analog to digital card. The computer used was a 386 Cacheperformer with a speed of 25 *MHz*. The card used was a Keithley-Metrabyte DAS-16F. The pump used to drive flow was a Sethco fiberglass centrifugal pump model CVR 1½x3x6. The pump speed is set with a Parametrics Parajust controller model G-04-200-A00. This pump could be connected to a calibration loop which consisted of a 150 gallon fiberglass recirculation tank, a 3-*in* suction line going to the pump and a 2-*in* discharge from the pump. The discharge line could either be directed into the calibration tank or the larger recirculation tank by operating two quarter-turn ball valves.

In order to monitor the hydraulic resistance of the test loop a Validyne model

DP15 variable reluctance differential pressure transducer was employed. Several diaphragms were used according to the maximum pressure difference which was expected to be measured. The transducer is operated in conjunction with a Validyne CD23 Digital Transducer Indicator, the output of which is 0 to 10 *V DC*.

Chapter 4

Experimental Procedures

4.1 Overview

The collection of the MHD thruster performance data entailed many preparatory experiments. Before any MHD experiments could be conducted at MIT, several procedures were undertaken at Penn State. The flowmeter and pressure transducer were calibrated and the hydraulic resistance of the loop was measured for various flowrates. Only following these experiments could thrust and efficiency be inferred from the flowrate. This chapter will discuss the procedures used in the above experiments as well as those used at MIT.

4.2 Flowmeter Calibration

A weight calibration of the flowmeter was performed using a 100 gallon neoprene tank, a portable Toledo weight scale, and a variable speed pump connected to a calibration line. The neoprene tank was placed on the weight scale. To begin each run, the 150 gallon recirculation tank was filled, the pump speed was set and the initial weight of the neoprene collection tank was recorded. Simultaneously, the data acquisition was started and the pump discharge was directed to the calibration tank. After a predetermined amount of time (60 *sec* for the very low flow rates, 30 *sec* for all others), the data acquisition would end and the pump discharge would be directed back to the recirculation tank. The data acquisition would monitor the 0 to 10 *V DC* output of the

flowmeter for the entire time, an average voltage and standard deviation would be calculated. The change in tank weight would be computed from which the change in volume could be calculated. From this information and the time interval the average volumetric flowrate, in *gpm*, could be calculated.

The above procedure was repeated three times per pump speed for pump speeds corresponding to many flowrates in the expected range. A least square, linear regression was performed on the recorded average voltages and volumetric flowrates following the collection of all of the data points. The results of the regression are used as input for the computerized data acquisition. Figure 4.1 shows the results of a sample regression of the EG&G Flow Technology Flowmeter.

4.3 Pressure Transducer Calibration

To begin the pressure transducer calibration the positive port of the transducer was connected to a known pressure source relative to atmospheric. Both a micromanometer or AMETEK pneumatic dead weight tester were used as pressure sources. The output of the Validyne CD23 was then connected to a computer which is configured for pressure calibrations.

At this point the zero and span of the of the CD23 were set by alternating zero and full scale pressure while adjusting the zero and span knobs until the desired voltages were obtained. After this the zero and span knobs were locked in place. Once this is done a set of points at zero pressure was recorded. Next a small known pressure was applied to the transducer. This pressure value was typed into the computer, after which

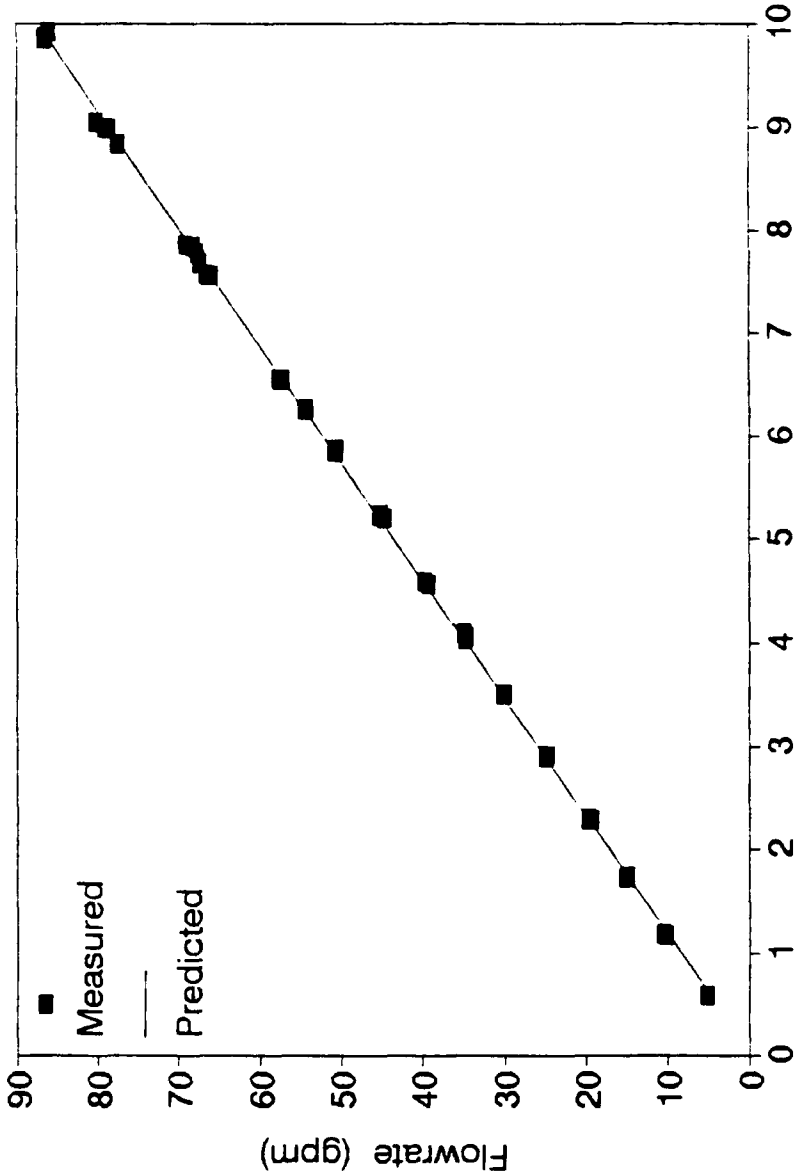

Figure 4.1 - Sample Graph of a Flowmeter Calibration

the computer automatically recorded the voltage from the CD23 unit. Several points were taken per pressure, typically three or four. This procedure was repeated for increasing pressures approximately 10 times. The micromanometer was used to generate pressures less than 20-*in of* H_2O and the AMETEK was used for the larger pressures.

The above procedure was repeated in reverse to account for any hysteresis in the transducer. All of the data was then used by the computer to obtain a linear relationship between pressure differential and CD23 voltage. Figure 4.2 shows the results of a sample pressure transducer calibration.

4.4 Determination of Hydraulic Resistance

To determine the hydraulic resistance of the test loop, the variable speed pump and a diaphragm valve were placed in the test loop at the flange connection immediately downstream of the test section. Pressure ports were placed as close to these flanges as possible. This placement of the pressure ports allows the pump and the plumbing between the pressure ports to be modelled as a perfect pump.

To begin the test, a flowrate was set by varying the pump speed and the position of the diaphragm valve. Once a flowrate had been established, the data acquisition system recorded the flowrate and pressure differential for a specified time. At the end of the test, the computer calculated the average and standard deviation for both the flowrate and pressure rise. This was repeated three times for each flowrate. Many different flowrates were examined within the expected flow range of the thruster.

This data is then fitted with a power law correlation. The power law was chosen

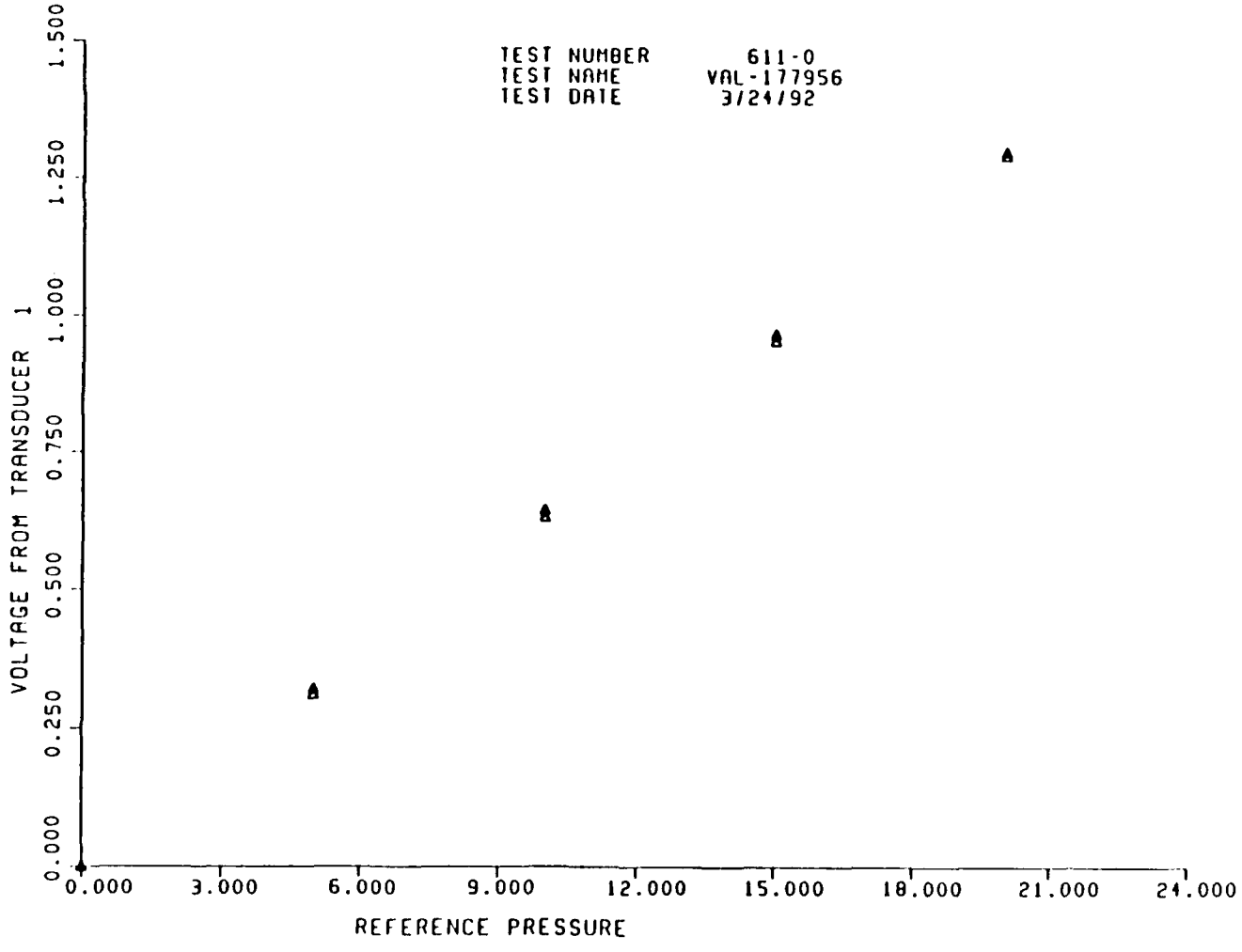

Figure 4.2 - Results from a Sample Pressure Transducer Calibration

because it gave the best fit of the experimental data. This information was then used to calculate the thrust generated by the test section from knowledge of the MHD induced flowrate as measured at MIT. These results will be presented in Chapter 5.

4.5 MHD Induced Flow Experiments

To begin the MHD induced flow experiments, the test loop was assembled and the tank was filled with 40 gallons of filtered water. Next the correct amount of "Sea-Salt" was added, and a mixer was placed in the solution. After the mixer had run for several minutes, the valves from the tank were opened and the auxiliary pump turned on. The pump was used to help mix and further filter the solution. After the solution was adequately mixed, the mixer was removed and the auxiliary pump was taken out of the loop. Temperature sensors, both resistive temperature detectors (RTD's) and thermocouples, and a gas venting line were then installed on the top of the tank. The RTD temperature sensors were calibrated at the beginning of each day.

Once the magnet was turned on, the experiments began in earnest. A magnetic field strength was set. Once this was done, a given electric potential or current was established. The earlier trips consisted of voltage controlled experiments, and the subsequent ones of current controlled experiments. For a given combination of magnetic field and current (or voltage), the data acquisition was used to take three data sets. Each data set consisted of 1100 points per monitored quantity, with the time difference between data points for a given channel being 10 *msec*. Once these three sets were taken a new current (or voltage) was established, and the process was repeated. Intermittently, the

auxiliary pump was used with the carbon activated filter to remove some of the electrolytic contaminants. This procedure of varying the current (or voltage) was repeated for a range of magnetic field strengths to the maximum value of 8.0 tesla.

It should be noted that the maximum magnetic field was only achieved on the first set of experiments. On other trips, the magnet had a audible "clicking" sound coming from its internals. Also several magnet current spikes were observed by the control room at the FBNML. Therefore, the maximum value for current through the windings was decreased to provide safer operation of the magnet.

Chapter 5

Steady State Experimental Results and Discussion

5.1 Overview

In order to evaluate the performance of the MHD thrusters, two trips were made to utilize the 8-T magnet at the FBNML. The first trip (January, 1992) was to examine the first variation of the circular test section. The second trip (April, 1992) was used to evaluate the performance of the second variation of the circular test section and the rectangular test section. The EG&G flowmeter was purchased in the time between the two trips and was used exclusively in the April experiments. The performance of this flowmeter was much better than the performance of the Data Industrial flowmeter.

The data in this chapter will be presented with an emphasis on the results of the second variation of the circular test section. The results from the first variation of the circular test section will also be presented in detail. Finally, the results of the rectangular test section will be covered.

5.2 Second Variation of the Circular Test Section

This test section is the optically improved version of the two circular test sections. A photograph of this test section is shown in **Figure 3.3**. The thruster is comprised of two 1-*in* wide, 5-*in* long electrodes oriented parallel to each other in a 2-*in* diameter channel. This variation also had a one inch shorter upcomer than the first variation.

5.2.1 Hydraulic Resistance of the Closed Loop

In order to be able to ascertain the gross thrust and operating efficiency of the test section a measure of the test loop's hydraulic resistance was made at different flowrates. The data points from this study were then curve fit using a power law form. The power law was chosen because the pressure drop in the loop should theoretically vary as the flowrate to a power between 1 and 2. The results of the hydraulic resistance calibration and the power law curve fit are shown in **Figure 5.1**.

As can be seen from the figure, the power law curve fit does a good job of estimating the hydraulic resistance of the test loop. The exponent in the power law form for this test section was 1.72, which is between the theoretical limits stated above.

5.2.2 Steady State Performance of the Second Variation, Circular Test Section

The steady state flowrate, thrust and mechanical efficiency curves for this test section are shown in **Figures 5.2-4**, respectively. These curves show the effect of electric current on the parameters of interest for different magnetic field strengths.

The measured flowrate curves (**Figure 5.2**) exhibit all of the characteristics theoretically predicted. The most noticeable trend is that for a given current the flowrate increases with increasing magnetic field strength. This is caused by an increase in the Lorentz force with increasing magnetic field strength. The second trend is the increase in flowrate with increasing current. Since the pressure rise in the thruster is linearly proportional to the applied current, the flowrate should be proportional to the current raised to the reciprocal of the exponent found in the hydraulic resistance curve (i.e.

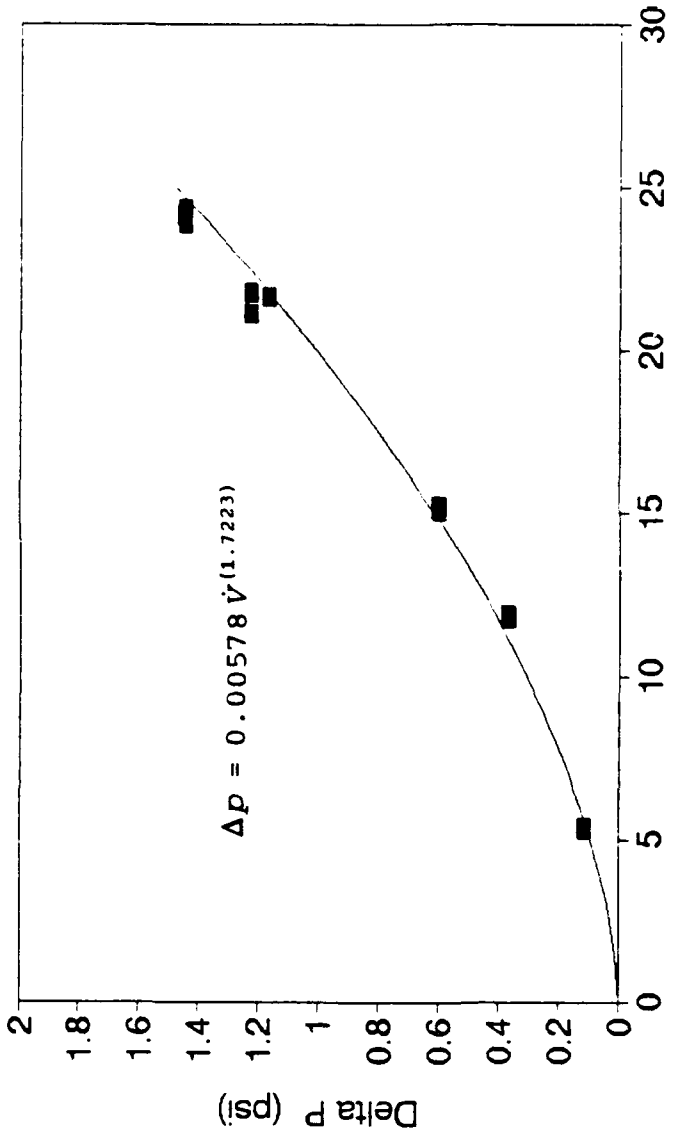

Figure 5.1 - Hydraulic Resistance of the MHD Test Loop with the Second Variation of the Circular Test Section

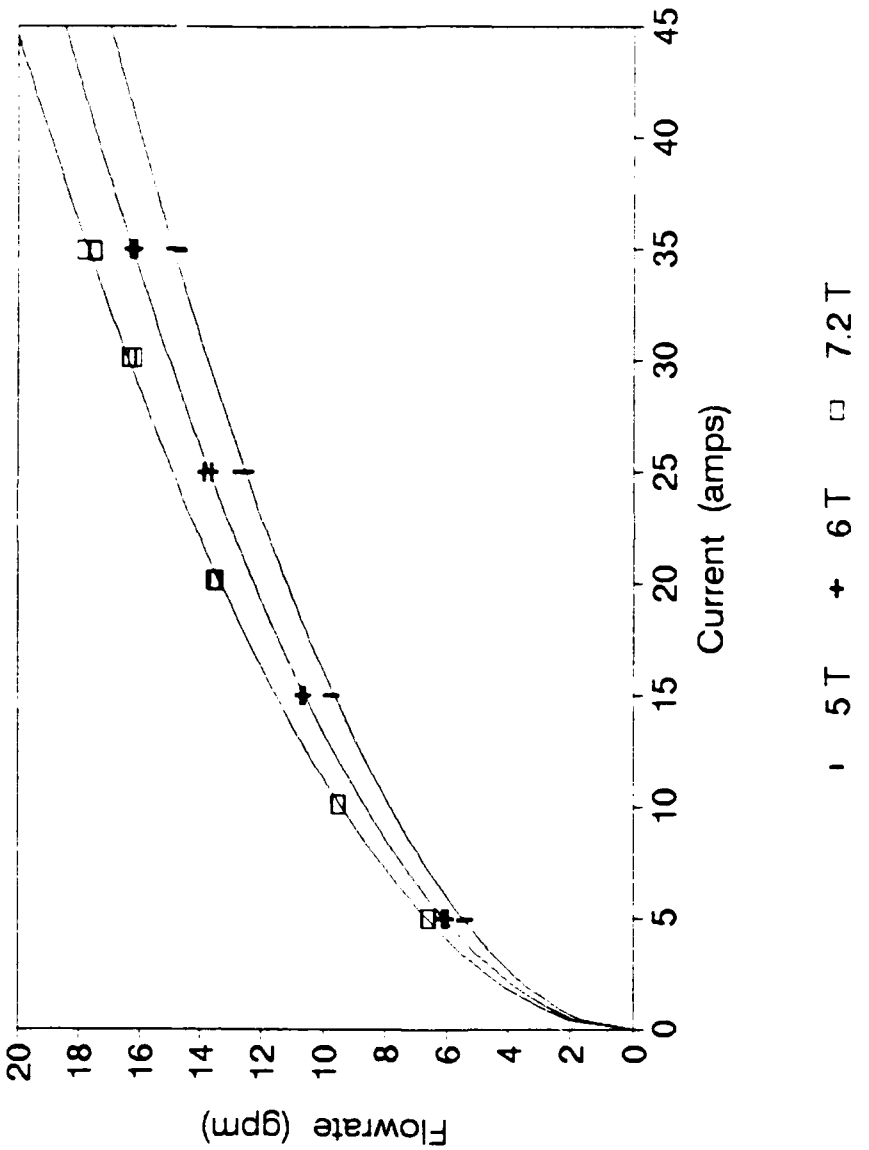

Figure 5.2 - Effect of Current on Flowrate for the Second Variation of the Circular Test Section

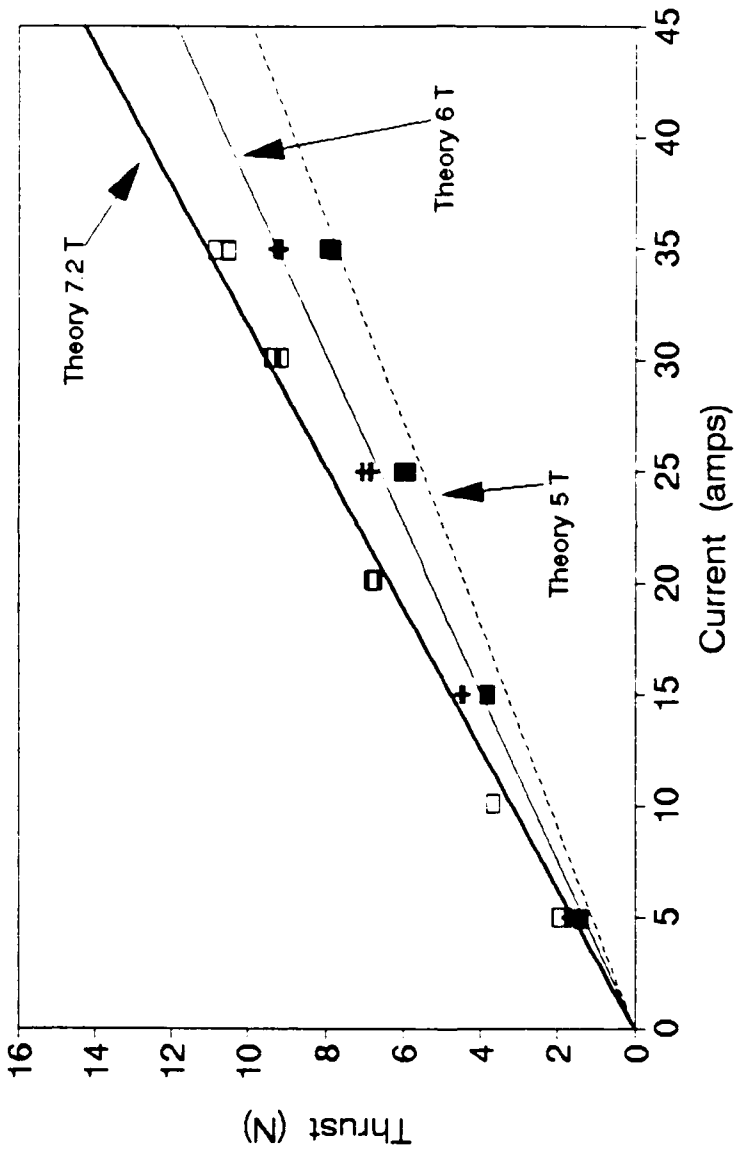

Figure 5.3 - Effect of Current and Magnetic Field Strength on the Thrust Produced by the Second Variation of the Circular Test Section

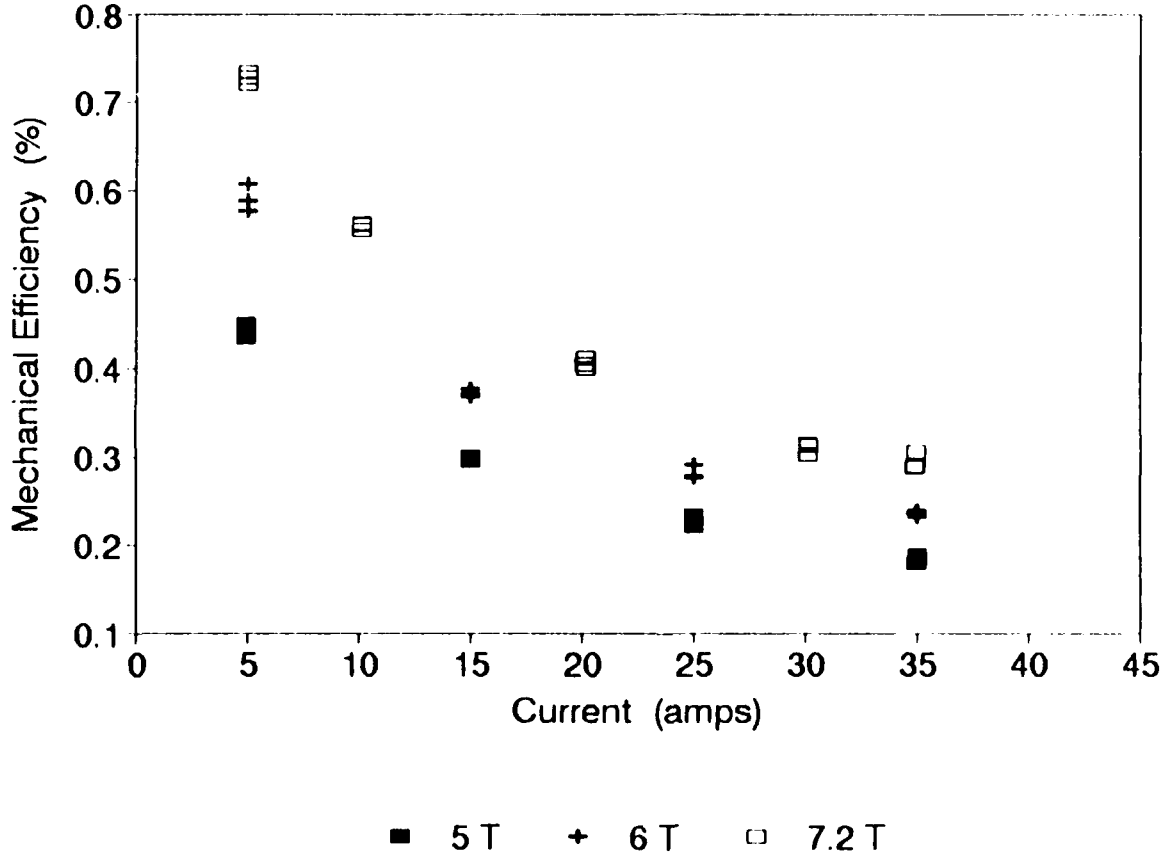

Figure 5.4 - Effect of Current and Magnetic Field Strength on Mechanical Efficiency for the Second Variation of the Circular Test Section

1/1.72). From a power law curve fit of the data the flowrate varies as the current raised to a power of approximately 0.51, depending on which magnetic field strength is examined. The best fit lines are also shown in **Figure 5.2**.

The next parameter of interest is the gross thrust produced by the test section. As can be seen in **Figure 5.3**, the thrust varies linearly with the applied current. This is the expected relationship based on **Eq. 2.2**. The measured/calculated thrust values agree well with the theoretical values. However, there are points at which the measured/calculated thrust exceeds the theoretical thrust. This phenomena can be explained by examining the method used to calculate the thrust. The thrust is determined from knowledge of the hydraulic resistance of the loop. Using a correlation relating the required pressure rise to cause a given flowrate, the MHD induced flowrates are measured and then the thrust is inferred. However, as the MHD induced flow experiments are conducted the water temperature is raised due to joule heating. The increase in temperature causes a slight decrease in the fluid viscosity which results in a slightly higher flowrate for a given pressure rise. The result is that the thrust calculated from knowledge of the flowrate is slightly overestimated. Temperatures rises on the order of 15°C were not uncommon in the course of the experiments. This temperature difference corresponds to $\approx 25\%$ decrease in viscosity.

Using the calculated thrust, a mechanical efficiency can be calculated using **Eq. 2.21**. The results of these calculations are shown in **Figure 5.4**. Again the curves show the expected trends. The most noticeable feature is the great increase in efficiency with increasing magnetic field strength. This is related to the linear relationship between thrust

and magnetic field strength. The other trend is that the efficiency decreases with increasing electric current. This is because the flowrate through the thruster varies with the current to a power less than one. Therefore when all of the terms in **Equation 2.21** for efficiency are expressed in terms of current, the efficiency will vary as current to a negative power (approximately $I^{-0.5}$).

Two dimensionless parameters often used to evaluate MHD thrusters are the Hartmann number and the interaction parameter. The Hartmann number is a measure of the pondermotive force to the viscous force in the thruster. The interaction parameter is a measure of the Lorentz force to the inertial force. The maximum value for the Hartmann number for this test section is 23.1 and the maximum value for the interaction parameter is 0.059. These values will not be given for the first variation of the test section due to the similarity in geometries.

5.2.3 Comparison of Code Predictions and Experimental Values

The computer code described in chapter 2 was used to predict the performance of the test section as a function of magnetic field strength, test loop configuration, and electric current. The two parameters of primary interest calculated by the code are the MHD induced flowrate and the thruster's mechanical efficiency. The comparison of flowrate for magnetic field strengths of 5 and 7.2 Tesla are shown in **Figure 5.5**. Both the measured and predicted values exhibit the same behavior, with predicted values consistently larger in magnitude. This can be explained by the fact the expansion and contraction losses in the code do not include two phase effects. This assumption causes

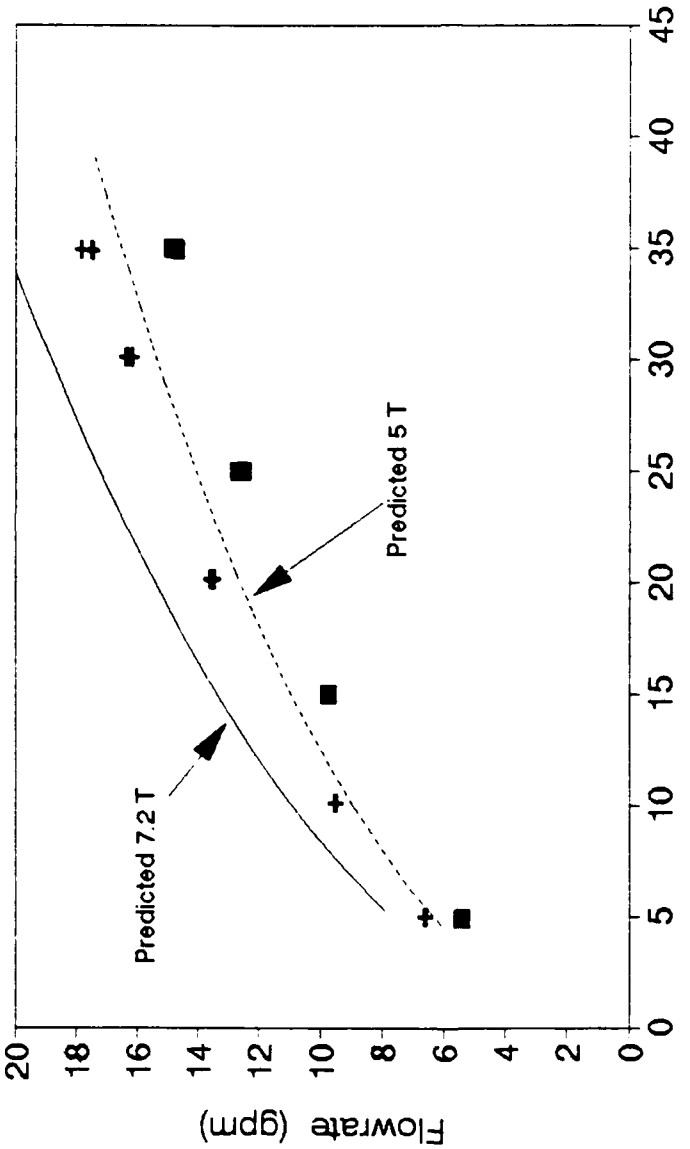

Figure 5.5 - Comparison of Predicted and Measured Flowrates for the Second Variation of the Circular Test Section

the contraction loss between the thruster and the upcomer to be underestimated. This pressure drop is a large part of the total loop pressure drop. This causes the slight overestimation in flowrate.

Predicted and measured/calculated values of mechanical efficiency are presented in **Figure 5.6**. The agreement between the two sets of data is very good. The magnitudes and shape of both sets are similar. This is somewhat due to discrepancies canceling each other out in computer code. The decrease in viscosity during the experiments was described above. This phenomena was offset by the temperature rise and electrolytic contamination increasing the conductivity of the seawater solution. Therefore the computer code would slightly overestimate the system flowrate, but would also overestimate the voltage requirements for a given current. These two factors would tend to cancel each other.

5.3 Results of the First Variation of the Circular Test Section

The data taken with the first variation of the circular test section exhibits many of the same characteristics as the second variation. The hydraulic resistance of the first variation is shown in **Figure 5.7**. As can be seen by comparing this graph to **Figure 5.1** this loop requires a larger pressure rise to induce the same flowrate. This is a result of the 1-*in* longer upcomer. Since the upcomer was only 1-*in* in diameter this resulted in a considerable decrease in the hydraulic resistance for the second variation. Likewise the hydraulic resistance of the Data Industrial flowmeter used in these experiments was greater than for the EG&G flowmeter used in the later studies.

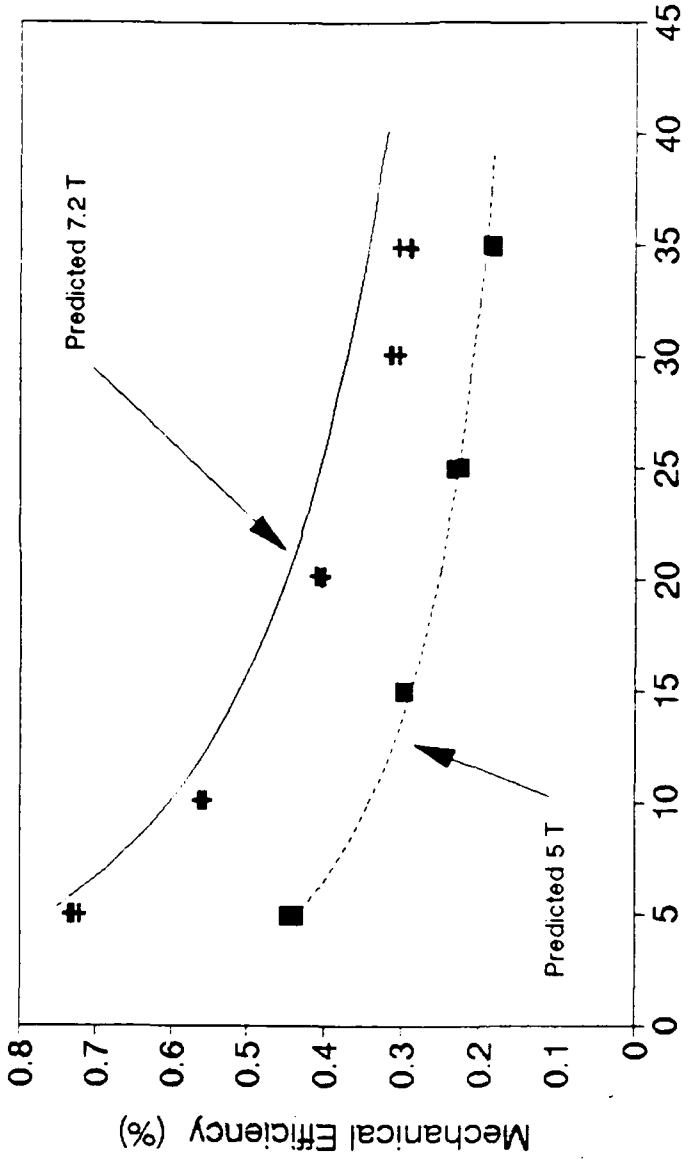

Figure 5.6 - Comparison of Predicted and Measured/Calculated Mechanical Efficiency for the Second Variation of the Circular Test Section

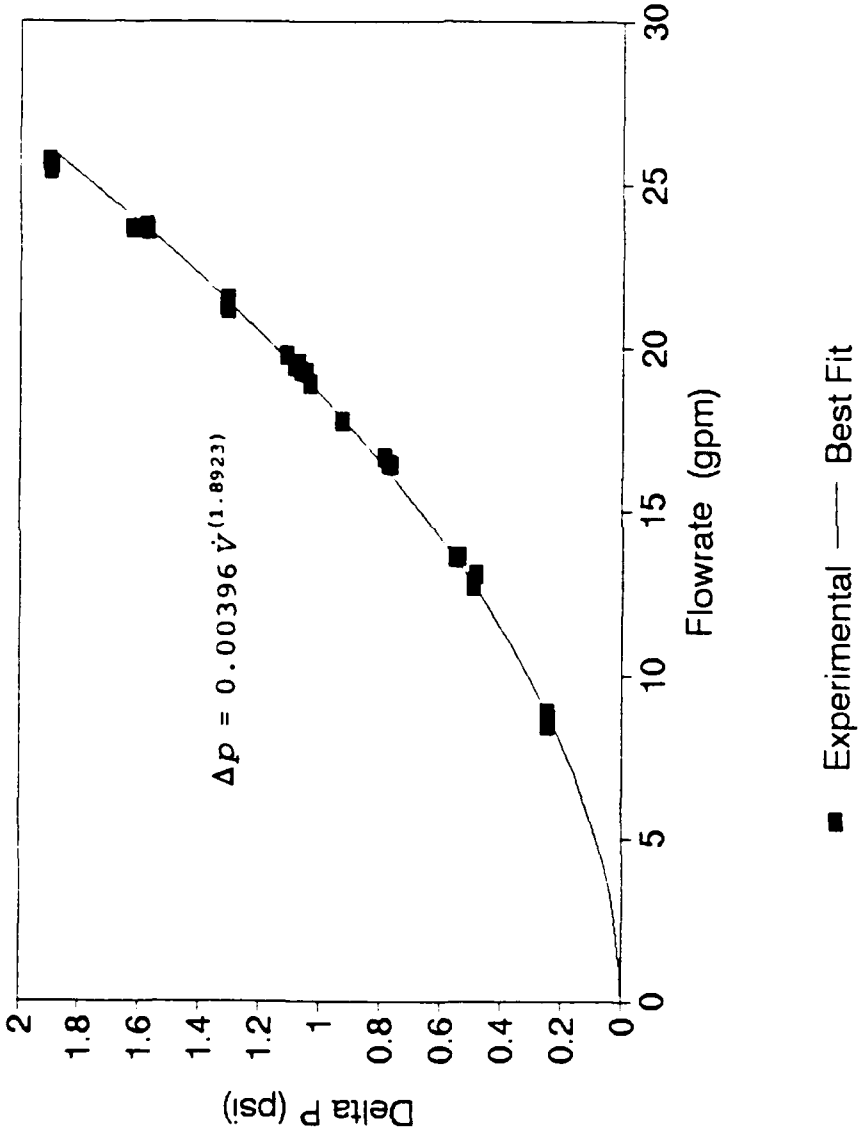

Figure 5.7 - Hydraulic Resistance of the First Variation of the Circular Test Section

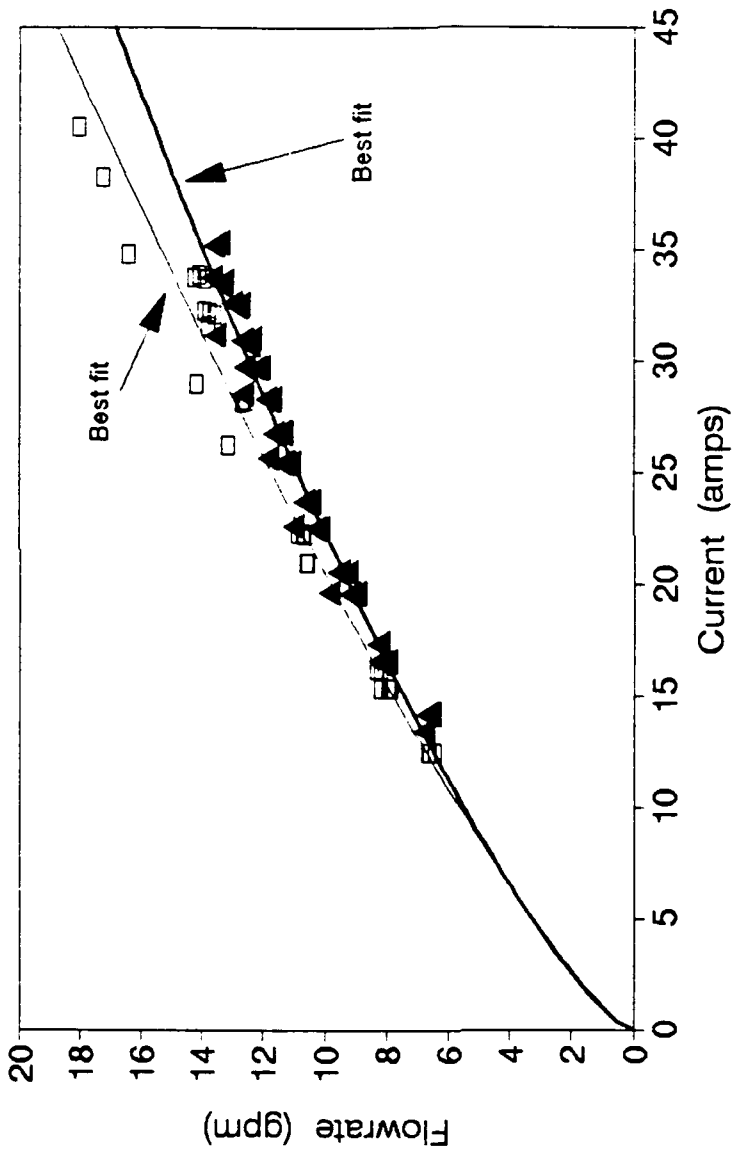

Figure 5.8 - Effect of Magnetic Field and Current on MHD Induced Flowrate for the First Variation of the Circular Test Section

Since the hydraulic resistance is increased for this test section, the flowrates should be slightly lower for the first variation. This can be verified when comparing **Figure 5.8** with **Figure 5.2**. From this comparison it can be seen that the flowrates from the second variation are indeed higher. When comparing these two graphs the increased accuracy of the EG&G flowmeter can be seen by the decreased spread in flowrate for a given current. Also the effect of using a current control can be seen as the points for the second variation are tightly clustered around specific currents. However, the first set of experiments was done by controlling the voltage which caused a variation in the currents as the conductivity of the seawater solution changed. Another difference between the two plots is the maximum magnetic field strength obtained. During the first trip to FBNML the full capacity value of 8 *Tesla* was achieved. However, problems with the magnet limited the maximum field strength in subsequent trips. The maximum value achieved in the second trip was 7.6 *Tesla*. Problems with the magnet at this field strength caused the field to be decreased before a full set of data could be obtained.

The three data points at the maximum current and flowrate can be attributed to an extremely warm seawater solution. The solution temperature for these runs was 30°C. This allowed for a larger current based on a given voltage and allowed the solution to be pumped more easily by decreasing the fluid viscosity.

The plot of the gross thrust produced by the test section (**Figure 5.9**) appears the same as for the second variation in both shape and magnitude. Again the spread in the data is more noticeable than for the second variation of the circular test section.

The graph of mechanical efficiency is shown in **Figure 5.10**. This plot shows

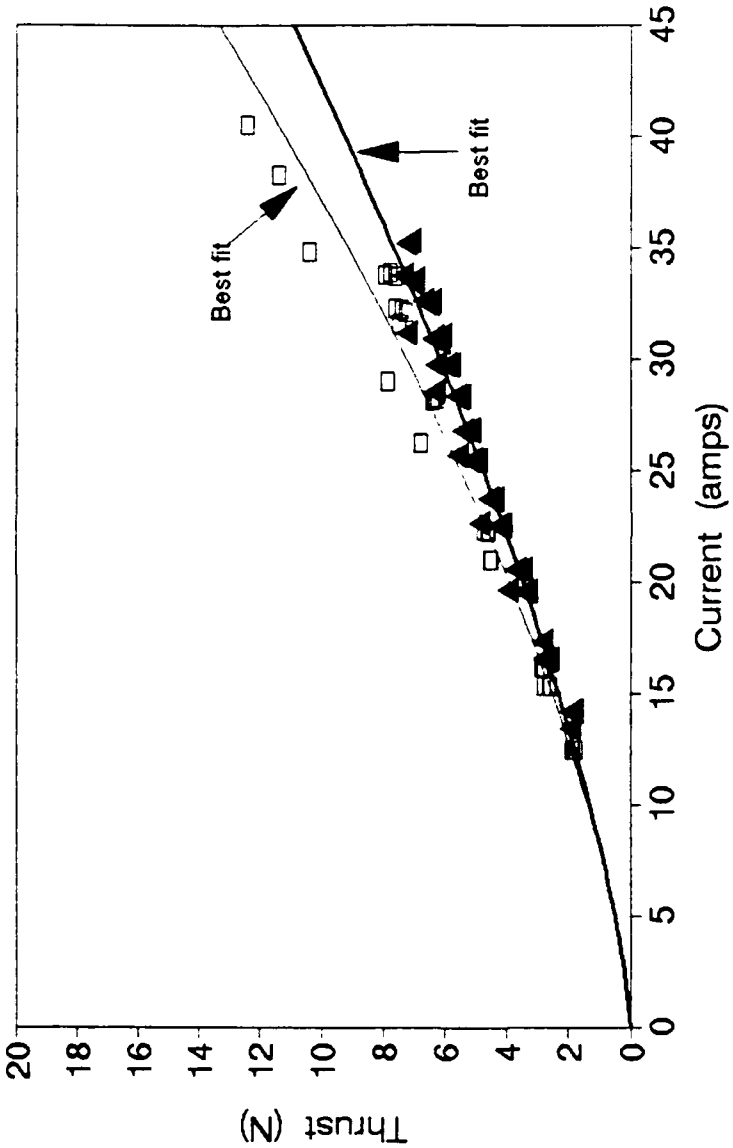

Figure 5.9 - Effect of Magnetic Field and Current on the Gross Thrust for the First Variation of the Circular Test Section

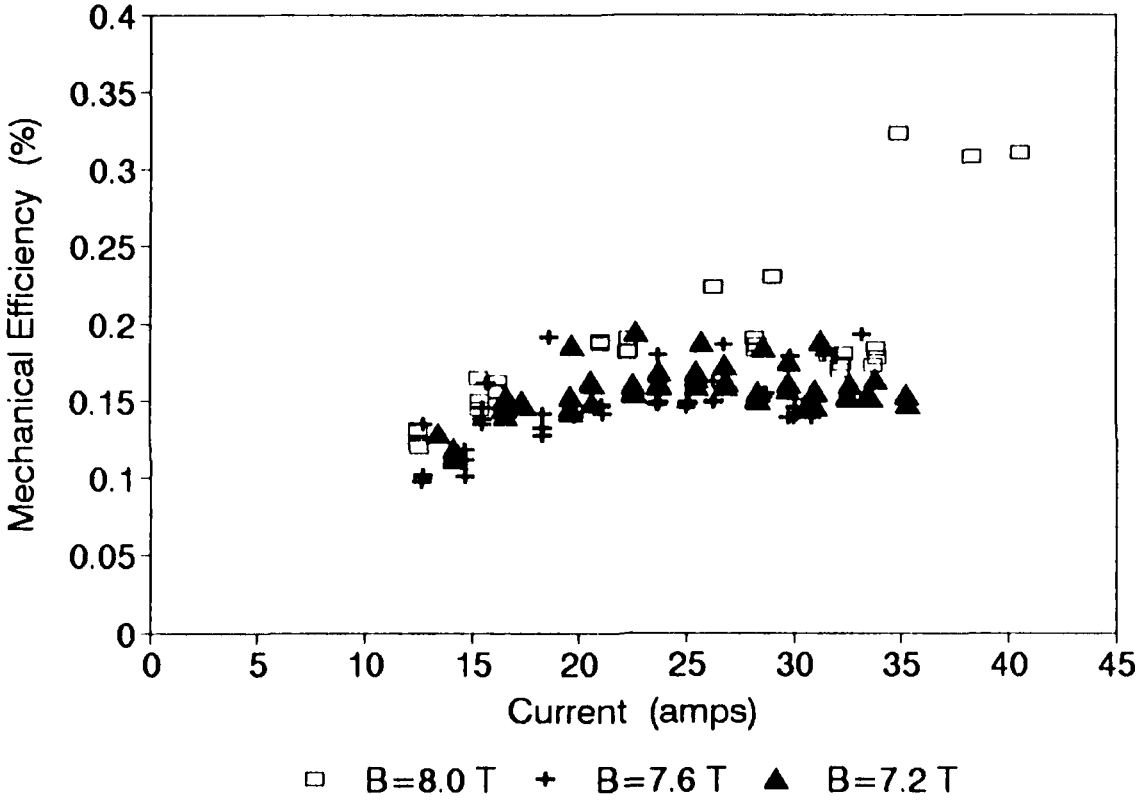

Figure 5.10 - Plot of Mechanical Efficiency of the First Variation of the Circular Test Section at Different Operating Conditions

considerable differences when compared to the efficiency plot for the second variation. The first difference is in the magnitude of the efficiencies. As a rule the efficiencies are much smaller for the first variation than the second for identical magnetic field strengths and currents. This can be explained by the decreased flowrate in the first variation.

The second difference between the two graphs is that there is no strong trend noticeable in the variation of efficiency with current. There are several possible explanations for this. The first is that the smallest current used in this case was 12 *amps*, by which point the second variation's efficiency had already dropped considerably. Therefore the part of the plot which most strongly shows the trend was not studied. Another possible explanation is that data was collected by establishing a magnetic field strength and then examining different voltages starting with lowest value and increasing voltage with each point. Since these experiments were performed with the Data Industrial Flowmeter, which had a very slow time response, the flow was allowed to stabilize for several minutes before taking data. Therefore, the heating of the water is more predominant for this test section and the electrical resistance could change enough to noticeably increase the efficiency between points. Since the efficiencies are so low, their values are more strongly tied to the electric power required by the thruster. Therefore, a small change in conductivity could cause significant change in the calculated efficiency. This problem did not occur for the second variation since the flowmeter had a response time of seconds and not minutes. Therefore, there was much less heating of the solution.

The final discrepancy between the two plots is that the effect of magnetic field strength is not clearly seen. Again this is attributed to experimental procedure. The data

for the 7.2 *Tesla* case was taken last. Therefore, the water was most conductive for this magnetic field strength, which causes artificially high efficiencies.

5.4 Steady State Results from the Rectangular Test Section

Since the plots of the interesting parameters for this test section are very similar in shape to those of the second variation of the circular test section, they will be omitted. This test section varied greatly in design from the circular test section. The larger electrodes caused a decrease in the electrical resistance. However, the larger electrodes caused the pressure rise in the thruster to be smaller for the same current. This occurred because the electrode gap remained the same but the flow area was increased by more than a factor of 6. This geometry coupled with the increase in upcomer diameter greatly decreased the hydraulic resistance of this test loop. The net result of the changes is that for a given current and magnetic field the flowrate in this test section was smaller than in the other thrusters. Also the decreased electrical resistivity was offset by the decreased fluid velocity. For comparison the maximum flowrate obtained in this test section was 21 *gpm* which was obtained with a current of 76 *amps* and a magnetic field strength of 7.8 *Tesla*. The decrease in resistance can be seen by the magnitude of current. The power supply used for this test section had a maximum voltage of 40 *VDC*, compared to 60 *VDC* for the power supply used to study the circular test sections. The maximum efficiency for this test section was 0.311% corresponding to 5 *amps* and 7.8 *Tesla*. The maximum value for the Hartmann number for this test section is 42.7. This value is substantially larger than for the circular test sections, and is due to the much larger

hydraulic diameter of this test section. The maximum interaction parameter is 0.54 which again is larger than that of the circular test section. This again is directly related to the increase in hydraulic diameter.

Chapter 6

Transient and Photographic Results

6.1 Overview

In a realistic setting the MHD thruster would need to increase or decrease its thrust output. As seen in the equations in Chapter 2 there are two ways to change the thrust produced by the test section. The first method is to change the electric current. To date this has been the only method studied due to the inability of a superconducting magnet to change its field strength. However, the magnets at the FBNML have the ability to change the current through the windings as a function of time. This ability was utilized to study the flowrate response to a changing magnetic field strength. The effects of changing electric current at a constant magnetic field strength were also studied.

All of the transient data presented was taken using the EG&G Flow Technology flowmeter due to its fast response. To provide comparison with graphs presented earlier, only data obtained from the second variation of the circular test section will be presented. The data for the rectangular test section exhibits the same trends as the data presented, only the magnitudes are slightly different.

Another advantage of using the 10-A magnet at the FBNML is that there is an optical pathway to observe the MHD pumping. This is the first time that this phenomenon has been either photographically or videographically recorded. A photograph of the MHD pumping will be presented and discussed.

6.2 Flowrate Response to Current Ramps

Through the use of a motor driven potentiometer the current through the test section was able to be changed as a linear function of time. To perform these experiments the magnetic field strength was set and the current was linearly ramped up or down. This type of transient would be the most likely method of changing the speed of an MHD driven vehicle.

The first example of a current ramp closely resembles the way in which an MHD thrust would start. In this example the magnetic field is set at 7.2 *Tesla*, and the current begins at 0 *amps* and is increased to 35 amps in 30 *seconds*. The flowrate response to this transient is shown in **Figure 6.1**. The trend in flowrate is as expected. Since there is a linear relationship between time and current, these curves would be expected to exhibit similar shapes as the flowrate versus current plots in chapter 5. Indeed this is the case. If the thruster were to act in quasi-steady state manner, the flowrate would begin to increase at the same time the current does. However, due to the inertia of the fluid there is a noticeable delay between the start of the current ramp and the first indication of flowrate response. For this example the delay appears to be approximately two seconds. It should be noted that flowrate indicated at the beginning of the ramp is incorrect. The flat portion of the curve before the increase in flowrate corresponds to no flow, since the flowmeter output was 0 *VDC*. This offset flow is an artifact of the linear flowmeter calibration which was performed. In order to force a zero *gpm* offset, the accuracy at the higher flowrates would have been comprised. This was an unacceptable situation, therefore a non-zero offset was used.

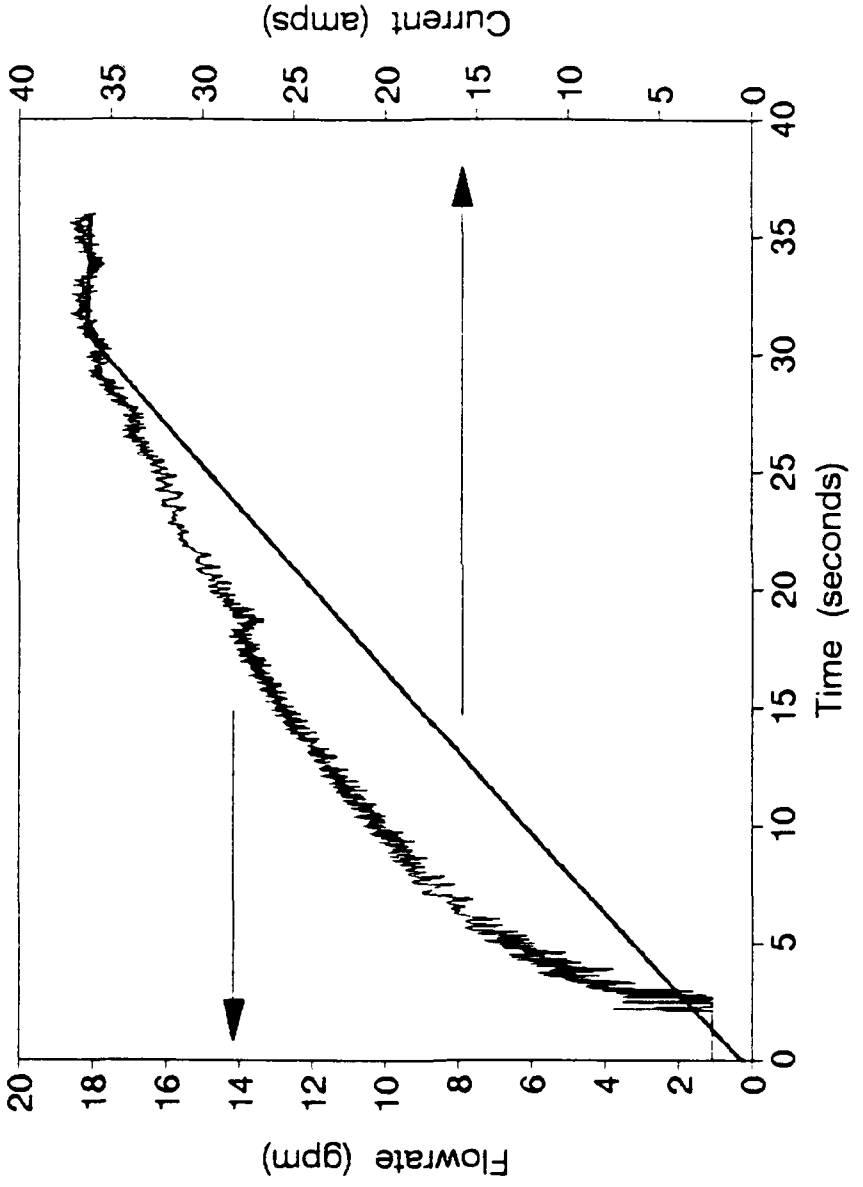

Figure 6.1 - Flowrate Response to a Linearly Increasing Electric Current for a B-Field of 7.2 *Tesla*

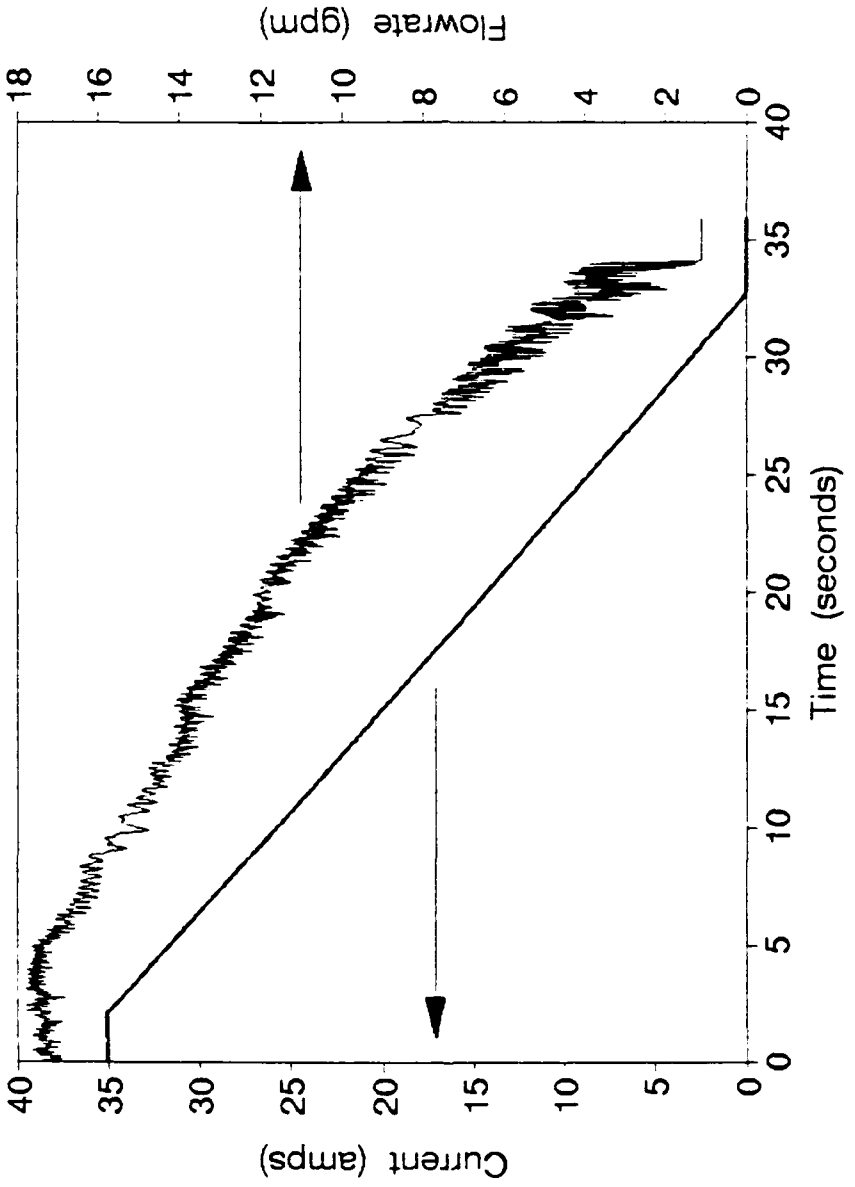

Figure 6.2 - Effect of a Linearly Decreasing Electric Current on Flowrate for a B-Field of *7.2 Tesla*

The next example simulates the MHD thruster being turned off. In this example, the magnetic field strength is again set to 7.2 *Tesla*, and the current is linearly ramped from 35 *amps* to 0 *amps*. The results of the transient are presented in **Figure 6.2**. This curve appears to be the mirror image to that of the increasing magnetic field case. Again, there is an appreciable time delay before the flowrate responds to the changing current. The response time for the decreasing current is approximately two seconds. This value is roughly the same value as for when the current was increasing. One interesting difference between the two graphs is the flowrate response at small currents. In the case of the upward ramp the flowrate curve had a much steeper slope than for the decreasing current. This can be attributed to the fact for the increasing current there is a force produced by the thruster which is attempting to increase the flowrate. On the other hand, when the current is decreased the thruster does not actively force the fluid to slow down from a state with higher flow inertia.

6.3 Flowrate Response to Magnetic Field Strength Ramps

The 10-A magnet at the FBNML has the ability to ramp the magnetic field strength at different rates. The magnetic field strength in this example was increased from zero to 7.2 *Tesla* in 30 seconds. The electric current for this case was 35 amps. Therefore, the final current and magnetic field strength for this example are the same as for the increasing current ramp which was presented above. The flowrate response to this B-field ramp is presented in **Figure 6.3**. This graph appears to be identical to the case of the increasing current ramp presented above. Both plots show the same steep flowrate

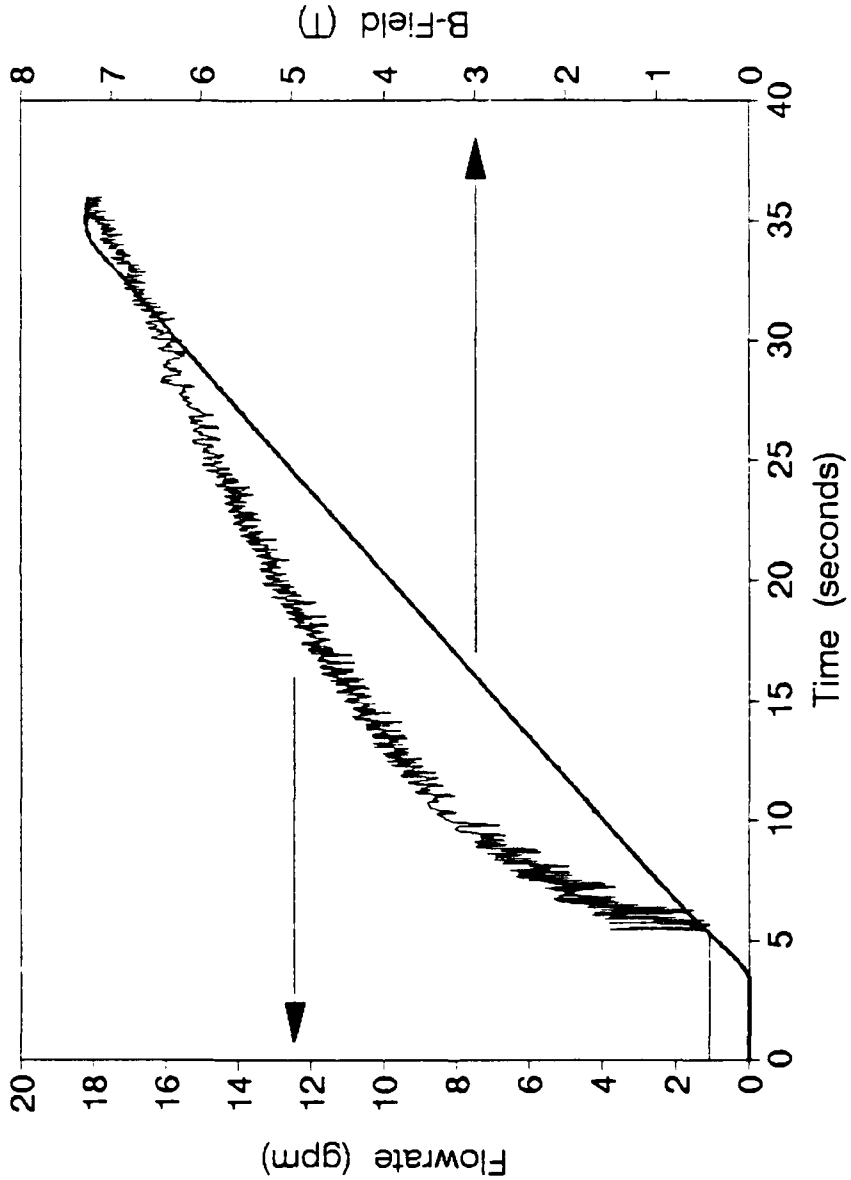

Figure 6.3 - Flowrate Response to Increasing B-Field Strength for a Current of 35 *amps*

increase in the beginning of the transient. The final flowrate for each of the examples is approximately 18 *gpm*. The similarity between the flowrate response to the current ramp and the magnetic field ramp was expected because both examples had the same rate of thrust increase.

6.4 Photographic Results

As stated above these experiments provided the first opportunity for researchers to view the two-phase MHD flow. A sample photograph is shown in **Figure 6.4**. In this photo the electric current of 30.1 *amp* is directed from the anode to the cathode. A magnetic field of 7.6 *Tesla* is directed into the photograph. Therefore, according to the right-hand rule the Lorentz force and induced flow is from right to left. This photograph was taken after the flowrate had reached its steady state value of 12.1 *gpm*. There appears to be an accumulation of the H_2 microbubbles at the end of the thruster. This is expected since the hydrogen is non-condensible. Therefore, since there is hydrogen production along the entire length of the cathode, the hydrogen concentration should increase toward the end of the thruster. The larger bubbles are believed to be the anode gasses of Cl_2 and O_2, both of which are somewhat condensible in the seawater solution. The jagged edge along the cathode is due to the build-up of a white jel-like substance. After chemical analysis this substance was determined to be a $Mg(OH)_2/Ca(OH)_2$ mixture. This material has never precipitated during previous seawater electrolysis experiments with these electrodes. Therefore, the presence of the magnetic field either increases the production of the precipitate by increasing the time in which the constituents spend in

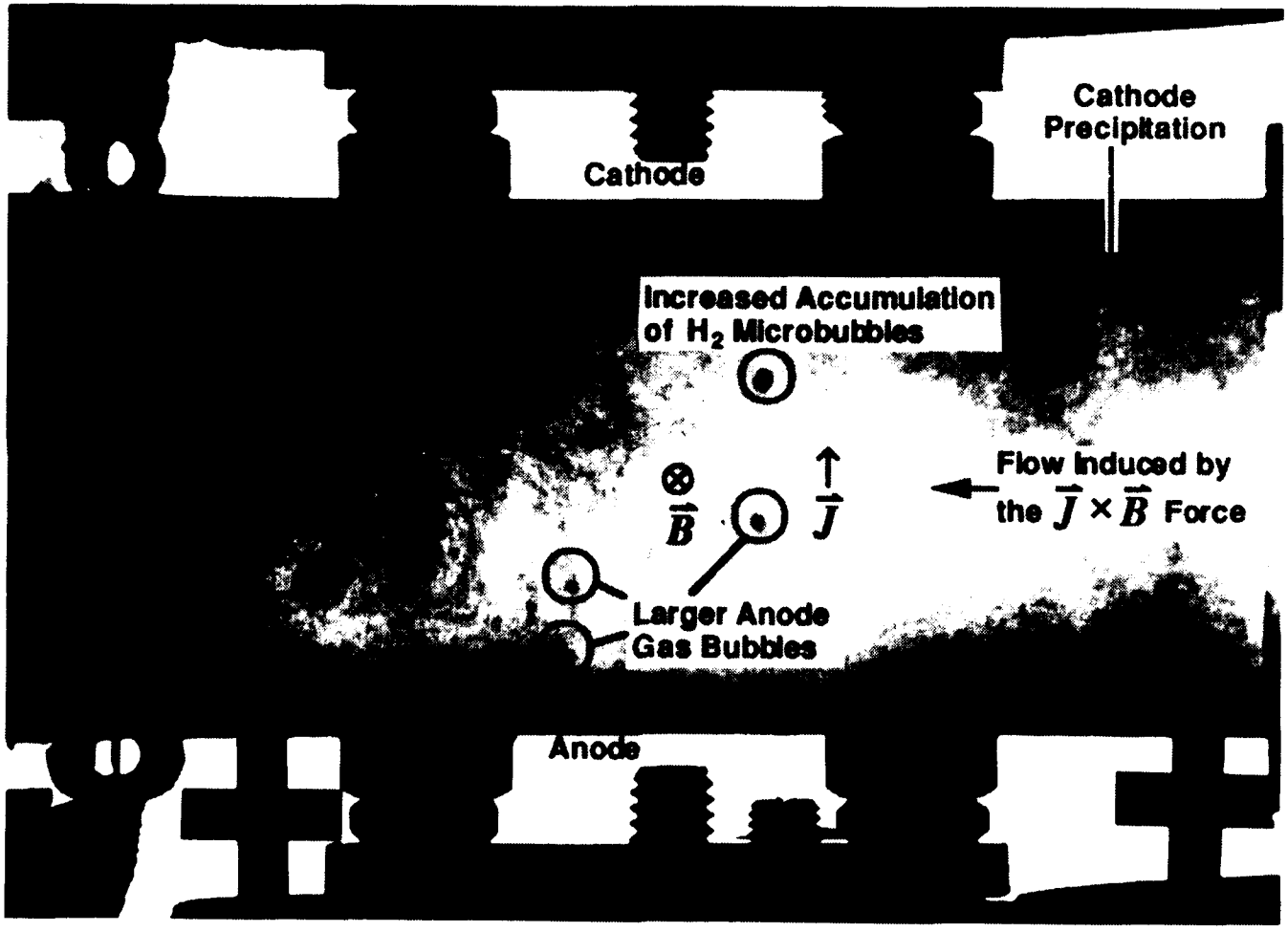

Figure 6.4 - Photograph of MHD Induced, Two-Phase Flow
(I = 30.1 *amps*, B=7.6 *Tesla*)

proximity to each other or the magnetic field causes the material to be held close to cathode long enough that the solution becomes supersaturated and begins to precipitate the $Mg(OH)_2/Ca(OH)_2$ mixture.

Chapter 7

Conclusions

7.1 Conclusions

During this work a predictive computer code was developed to model the performance of an MHD thruster in a closed loop environment. This code was used to optimize the geometry of the MHD test sections. Three different test sections were designed, constructed and evaluated. The results of these experiments were used as a benchmark for the computer code. It was shown that the code did a good job of estimating the flowrate, thrust and efficiency of an MHD test section at different magnetic field strengths and electric currents.

Data was taken and analyzed for both steady state and transient operating conditions. The flowrate, thrust and efficiency exhibited the predicted trends with variations in both electric current and magnetic field strength.

Using the 10-A magnet of the FBNML, the highest magnetic field (8 *Tesla*) among all research groups in the world for MHD propulsion was utilized. This solenoid magnet allowed visual access to perform videographic and photographic recordings of the two-phase MHD induced flow.

This research has shown that MHD propulsion is a viable form of undersea propulsion. The experiments have also shown the need for more research to improve the performance of these thrusters.

7.2 Future Considerations

In order to make MHD propulsion a more attractive alternative the efficiency must be increased. The primary reason for the low efficiencies in this study is the short thruster length. If the effective length of the thruster could be increased the efficiency would be improved. One method of achieving this goal is to go away from a system in which the current and flow are orthogonal in a cartesian coordinate system and instead use a cylindrical system.

Two types of cylindrical systems have been proposed. The first plan uses discs with a radial current and axial magnetic field to induce an azimuthal flow. Using this method several loops could be joined together to add additional length to the thruster. This concept has recently been tested by this group. A photograph of a single-loop thruster is shown in **Figure 7.1**. The preliminary results are very promising. A maximum flowrate of approximately 45 *gpm*, and a maximum efficiency of 6% were achieved. **Figure 7.2** compares the efficiencies for the single-loop and two-loop systems as a function of current.

Another approach is to use a helix design which would allow for a very smooth transition between the different loops. This design is currently being analyzed using a slightly different version of the computer code than that used for the test sections described in this paper. A listing of this code can be found in **Appendix B**.

The photographic recordings have shown the MHD induced flows to be two-phase. Therefore a determination of the void fraction within the test section must is necessary. The presence of the gasses decreases the performance of the thruster by

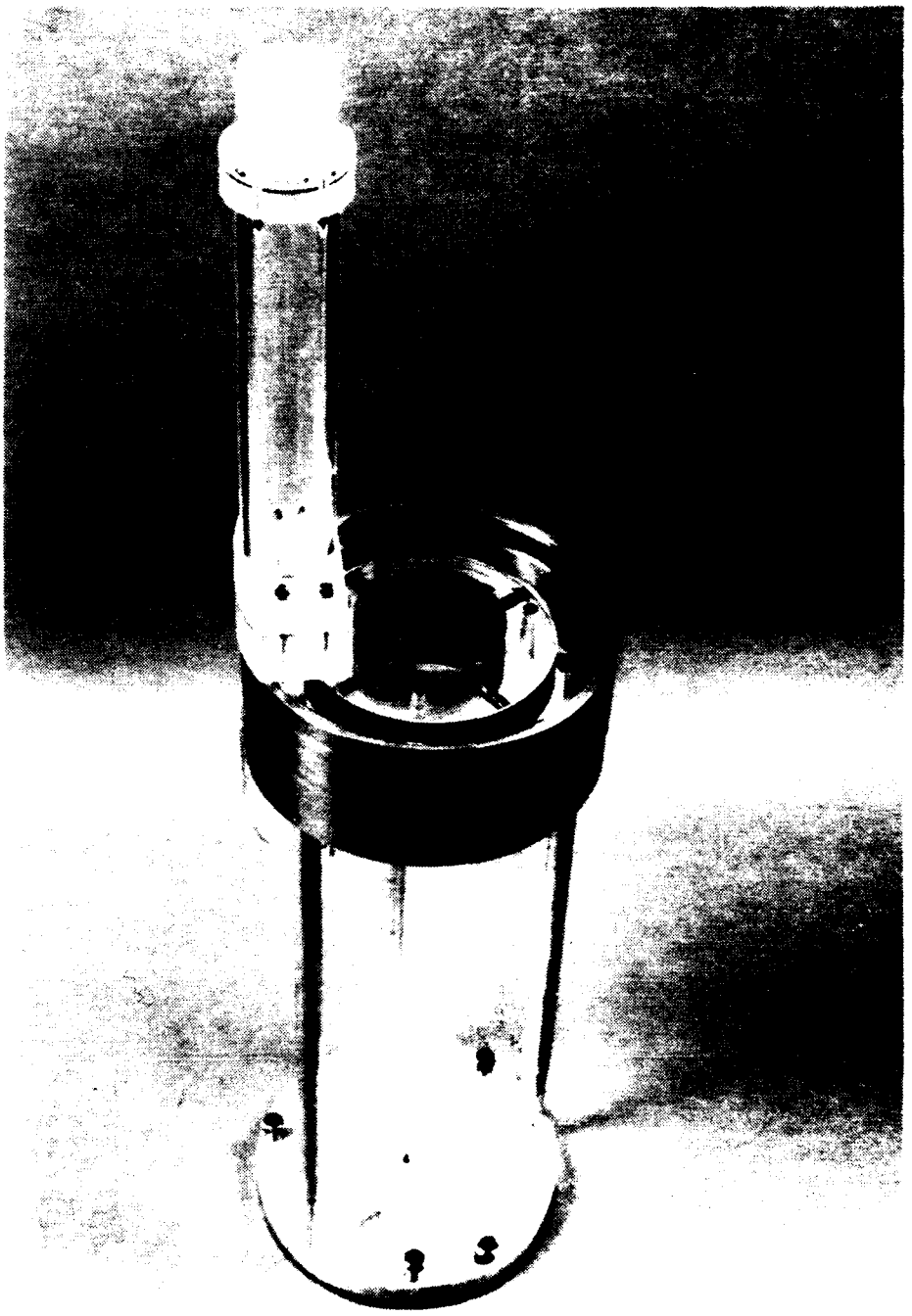

Figure 7.1 - Photograph of the MHD Cyclotron Thruster Design

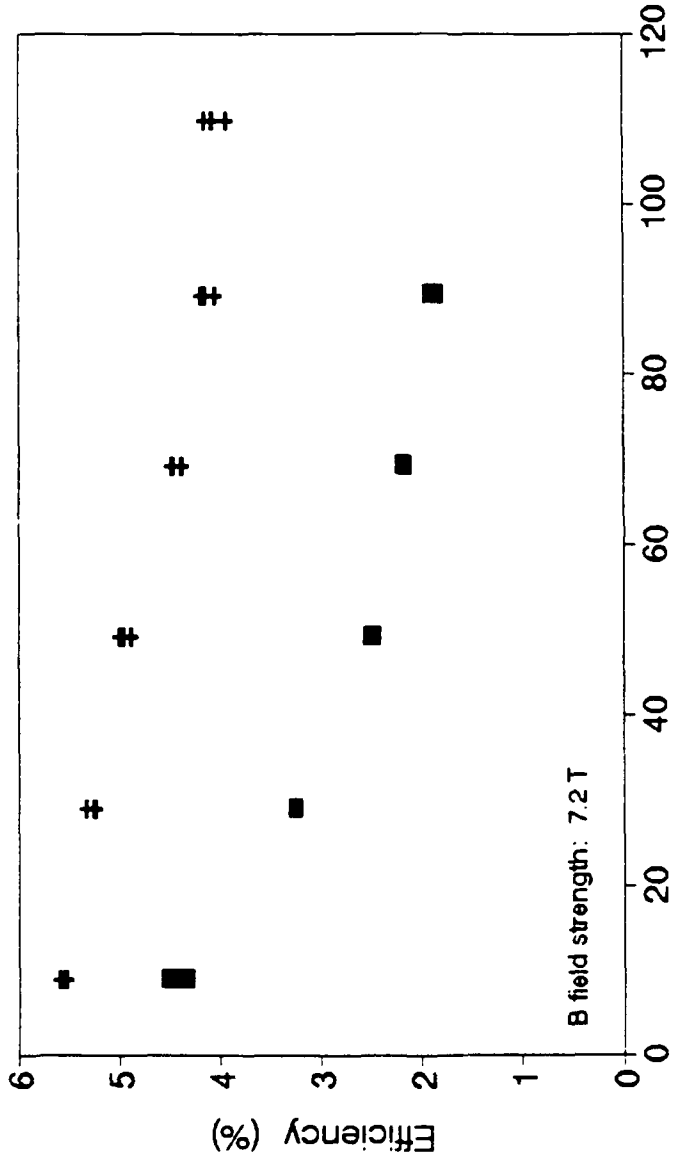

Figure 7.2 - Comparison of Efficiencies for a One- and Two-Loop Thrusters for Different Currents

increasing the electric and hydraulic resistance of the test section. Therefore a theoretical model which describes the rate at which chlorine dissolves into seawater and/or an experimental determination of the void fraction should be developed.

REFERENCES

1. T.F. Lin, "Superconducting Magnetohydrodynamic Ship Propulsion - A Worldwide Research Effort," *Scientific Information Bulletin, Office of Naval Research Asian Office*, vol. 17, no. 3, 1992, pp. 237-242.

2. S. Motora, K. Imaichi, M. Nakato, and S. Takezawa, "An Outline of the R&D Project on Superconducting MHD Ship Propulsion in Japan," Proceedings from MHDS 91, International Symposium on Superconducting Magnetohydrodynamic Ship Propulsion, October 1991, pp. (1-1-1) - (1-1-13).

3. J.B. Gilbert, **Feasibilty Study of the Magnetohydrodynamic Thruster for Marine Vehicle Applications**, Penn State Master's Thesis, 1990, pp. 32-36.

4. J.B. Gilbert and T.F. Lin, "Studies of MHD Propulsion for Underwater Vehicles and Seawater Conductivity Enhancement," ONR Annual Report, Feb. 1991, pp. 91-105.

5. J. Naggar, "Electrolysis Phenomena of Flowing Simulated Seawater for Magnetohydrodynamic Applications," Penn State Honor's Thesis, 1991, pp. 10-26 and 48-59.

6. S. Marks, **Study of The Multiphase Structure in Electrolytic Seawater Flows**, Penn State Master's Thesis, 1991 pp 6-19 and 37-41.

7. T. Imblum "Private Communications", May 1, 1991.

8. Crane Company, **Flow of Fliuds Through Valves, Fittings and Pipe (Metric Edition)**, 1986, pp. A28-A29.

9. F.P. Incropera and D.P. De Witt, **Fundamentals of Heat and Mass Transfer**, John Wiley and Sons, 1985, p. 372.

Appendix A

COMPUTER CODE USED TO PREDICT PERFORMANCE OF A LINEAR THRUSTER

```
Program MODU;
{$R+}
{$S-}
{$M 8192,0,0}
uses crt,Dos;

{All units will be in SI units}

Const
  Sigma = 5;
  nu    = 1.181e-6;
  rho   = 1025;
  tol   = 0.001;
  kin   = 0.5;
  kout  = 1;
  vf    = 1/rho;
  C_Cl  = 3.6809E-7;          {To make alpha = 0 put squiggly lines}
  C_H   = 1.0464E-8;          {around these lines and remove them}
 { C_Cl = 0;}                  {these}
 { C_H = 0;}                   {lines}
  rho_H = 0.0837;
  rho_Cl = 2.9944;
  Vo = 2.25;

  Gc    = 9.81;

Var
  D_ele,                {Inner Diameter of test section tubing}
  W,                    {Width of the electrodes}
  D,                    {Distance between electrodes}
  L_ele,                {Length of the electrodes}
  A_ele,                {Cross-Sectional flow area of test section}
  p,                    {Wetted perimeter of test section}
  Dh_ele,               {Hydraylic Diameter of test section}
  L1pa,                 {Length of vertical PVC   on bottom half of loop}
  L1pb,                 {Length of horizontal PVC "    "     "   "    " }
  D1p,L1p,A1p,          {Inner Diameter, Length, Area of lower PVC pipe}
  D2p,L2p,A2p,          {  "      "       "      "   "  upper  "   "  }
  D1t,L1t,A1t,          {  "      "       "      "   "  lower tygon tubing}
  D2t,L2t,A2t,          {  "      "       "      "   "  upper   "      "  }
  D1a,L1a,A1a,          {  "      "       "      "   "  lower acrylic tubing}
  D2a,L2a,A2a,          {  "      "       "      "   "  upper    "      "   }
  theta,                {Angle Characteristic of the electrode width}
  R,                    {Electrical Resistance which the electrodes see}
  U,                    {Water Velocity through the test section}
  Re,                   {Reynolds # of the flow in the test section}
  I,                    {Electrical current through the test section}
  V,                    {Voltage difference between the electrodes}
  eta,                  {Induction efficency for the test section}
  gpm,                  {Flow rate through the test section in GPM }
  B,                    {Magnetic Field Strength}
  Rt,                   {Total two phase multiplier}
  M_H,                  {Mass production rate of Hydrogen}
  M_Cl,                 {  "       "       "   "  Chlorine}
  Chi_TS,               {Mass percentage of Gas in the Test Section,
                         Quality}
  vg,                   {equivilent specific volume of gas phase}
  eta1                  {% of undissolved Cl in test section},
  eta2,                 {" "      "       " "  return acrylic}
  eta3,                 {" "      "       " "    "    tygon}
```

```
  eta4,                {" "      "        " "    "    PVC}
  Kcon1,               {from 2 in PVC to  2 in TYGON}
  Kcon2,               {from 2 in Tygon to 1.75 in Acry}
  Kexp1,               {from 1.75 Acry to 2 in Lexan}
  Kcon3,               {from 2 Lexan to 1 in Acryl}
  Kexp2,               {from 1 Acryl to 2 Tygon}
  Kexp3                {from 2 Tygon to 2 PVC}                  : Real;

  count        : Integer;
  outfile      : text;
  outname      : string[15];
  temp         : string[20];
  command      : string[50];
  letter       : char;
  flag         : boolean;


{*************************************************************************}
{*************************************************************************}
{*************************************************************************}

{Function vg:real;

  This function calculates the specific volume of the 'equivelent gas'

Var
  vg_temp : real;


Begin
  vg_temp:= ((1/rho_h) + (1/rho_Cl))/(2);
  vg := vg_temp;
End;}

{*************************************************************************}
{*************************************************************************}
{*************************************************************************}

Function alpha(X : real):real;

  {This function calculates the void fraction given a quality}

VAR
 al_temp : real;

Begin

  If (X<=0) then
    al_temp := 0
  else
    al_temp := 1/(1+((1-X)/X)*(vf/vg));
  alpha := al_temp;
End;

{*************************************************************************}
{*************************************************************************}
{*************************************************************************}

Function dpa(U,X : real):real;
```

```
{*************************************************************************}
{*************************************************************************}

Function dplph(U,Di,L:Real):Real;

{This function calculates the 1 phase frictional pressure drop}

Var
  Re,
  Temp_dp : Real;


Begin
   Re := U*Di/nu;
   temp_dp := f(Re)*(L/Di)*U*rho*U/2;
   dplph := temp_dp;
End;



{*************************************************************************}
{*************************************************************************}
{*************************************************************************}
Procedure GetI(Var I1: real;I_large,Ismall,U_TS,V_ele : real);

  Var
    I2 : Real;
    difference : real;
    M_H, M_CL_init,Chi_i,mdot : real;
    mg : real;

Begin
   Repeat
     I1 := (I_large+ISmall)/2;
     mdot := A_ele*rho*U_TS;
     M_H  := C_H*I1;
     M_Cl_init := I1*C_Cl;
     M_CL := eta1*M_Cl_init;
     mg := M_H + M_Cl;
     Chi_i:= mg/mdot;
     R := D/(W*L_ele*1.7092*sigma*(1-alpha(Chi_i)));
    { R := D/(W*L_ele*1.7092*sigma);}
     I2 := (V_ele-Vo-B*U_TS*D);
     I2 := I2/R;
     difference := (I1 - I2)/I1;
     If (difference <0) then
       Begin
         I_large:= I2;
         Ismall := I1;
       End
     Else
       Ismall := I2;
       I_large := I1;
  until (Abs(difference)<tol);
End;
```

```
          {This function calculates the acceleration pressure drop}

VAR
  G,              {Mass flux}
  dpa_temp,
  temp1,temp2 :real;

Begin
  G := rho*U;
  If (X=0) then
    dpa_temp := 0
  else
    Begin
      temp1 := vf*((1-X)*(1-X)/(1-alpha(X)) - 1);
      temp2 := vg*(X*X)/alpha(X);
      dpa_temp := (G*G)*(temp1 + temp2);
    End;
  dpa := dpa_temp;
End;

{*************************************************************************}
{*************************************************************************}
{*************************************************************************}


Function Rf(X:real):real;

  {This function calculates the 2 phase friction multiplier}

VAR
  Rf_temp,
  beta : real;

Begin
  beta := 1/(1-alpha(X));
  Rf_temp := (1/3)*(1+ beta + beta*beta);
  Rf := Rf_temp;
End;

{*************************************************************************}
{*************************************************************************}
{*************************************************************************}


Function f(Rey:real):real;

{This function calulates the friction factor}

VAR
  f_temp : real;

Begin
  if (Rey <= 2300) then f_temp:= 64/Rey
    else if (Rey <= 2e5) then f_temp := exp(ln(0.316) - 0.25*ln(Rey))
      else f_temp:=exp(0.184-0.2*ln(Rey));
  f:=f_temp;
End;


{*************************************************************************}
```

```
{*************************************************************************}
{*************************************************************************}
{*************************************************************************}
Procedure GetU(Var Uin, Iu, etau : Real ; small,large,Vu : real);

{This procedure does all of the iterations to find the correct velocity}

  Var
    dpf_ele,dpf1a,dpf2a,
    dpf1p,dpf2p,dpf1t,dpf2t,
    dpf,dpfa,dpfp,dpft,
    dpend1,dpend2,dpend,
    prise,diff,I_start,I_end,
    M_H,mdot_tot,
    M_Cl,M_Cl_init,Chi,
    U1p,U2p,U1a,U2a,U1t,U2t      : Real;
    ch      : char;

Begin
  Uin :=  (small+large)/2;
  etau := (Uin*B*D)/Vu;
  mdot_tot := Uin*A_ele*rho;
  GetI(Iu,400,0,Uin,Vu);
  M_H  := C_H*Iu;
  M_Cl_init := Iu*C_Cl;
  M_CL := eta1*M_Cl_init;
  Chi := (M_H+M_Cl)/mdot_tot;

  dpf_ele := Rf(Chi)*dp1ph(Uin,Dh_ele,L_ele+60*Dh_ele);
  dpf_ele := dpf_ele + dpa(Uin,Chi);

  U1p :=(A_ele/A1p)*Uin;
  dpf1p  := dp1ph(U1p,D1p,L1p);
  U2p := (A_ele/A2p)*Uin;
  M_Cl := eta2*M_Cl_init;
  Chi := (M_H+M_Cl)/mdot_tot;
  dpf2p := Rf(Chi)*dp1ph(U2p,D2p,L2p) + dpa(U2p,Chi) ;
  dpfp := dpf1p + dpf2p;

  U1t := (A_ele/A1t)*Uin;
  dpf1t  := dp1ph(U1t,D1t,L1t) + Kcon1*U*U*rho/2;
  U2t := (A_ele/A2t)*Uin;
  M_Cl := eta3*M_Cl_init;
  Chi := (M_H+M_Cl)/mdot_tot;
  dpf2t := Rf(Chi)*(dp1ph(U2t,D2t,L2t)+Kexp3*U2t*U2t*rho/(2)) + dpa(U2t,Chi);
  dpft := dpf1t + dpf2t;

  U1a := (A_ele/A1a)*Uin;
  dpf1a  := dp1ph(U1a,D1a,L1a) + (Kcon2+Kexp1)*U1a*U1a*rho/(2);
  U2a := (A_ele/A2a)*Uin;
  M_Cl := eta4*M_Cl_init;
  Chi := (M_H+M_Cl)/mdot_tot;
  dpf2a := Rf(Chi)*(dp1ph(U2a,D2a,L2a) + (Kexp2+Kcon3)*U2a*U2a*rho/(2));
  dpf2a := dpf2a + dpa(U2a,Chi);
  dpfa := dpf1a + dpf2a;

  dpf  := dpf_ele + dpfp + dpft + dpfa;

  dpend1 := kin*rho*U1p*U1p/2;
  dpend2 := kout*rho*U2p*U2p/2;
```

```
  dpend  := dpend1+dpend2;


  prise  := (Iu*B*D)/A_ele;
  diff   := (prise - dpf - dpend)/(prise);
  if (abs(diff)>tol) and (diff<0) then
  GetU(Uin,Iu,etau,small,Uin,Vu)
    else if (abs(diff)>tol) and (diff>0) then GetU(Uin,Iu,etau,Uin,large,Vu)
      else
end;

{*****************************************************************************}
{*****************************************************************************}
{*****************************************************************************}

Begin  {Main Program}
  repeat
    clrscr;
    temp := '72tesla';
    outname :=  temp +'.dat';
    assign (outfile,outname);
    command := 'print '+ outname;
    rewrite (outfile);

    vg := ((1/rho_h) + (1/rho_Cl))/(2);
    B := 7.2;
    W := 1*0.0254;

    D1p := 2.067*0.0254;
    D2p := 2.067*0.0254;
    D1t := 2*0.0254;
    D2t := 2*0.0254;
    D1a := 1.75*0.0254;
    D2a := 1.00*0.0254;
    D_ele := 2*0.0254;

    L1a := 10*0.0254;
    L2a := 10*0.0254;
    L1pa := (21*0.0254)*1.02;
    L1pb := (53*0.0254)*1.02;
    L1p := L1pa + L1pb + 63*D1p;
    L2p := (34*0.0254)*1.02 + 3*D2p;
    L1t := 24*0.0254;
    L2t := L1t-12*0.0254;
    L_ele := 5*0.0254;

    eta1 := 1.00;    {This will need to be changed to study effect}
    eta2 := 1.00;    {of chlorine production}
    eta3 := 1.00;
    eta4 := 1.00;

    D := 2*sqrt((D_ele*D_ele)/4 - (W*W)/4);
    theta := 2*arctan(D/W);
    A1p := Pi*D1p*D1p/4;
    A2p := Pi*D2p*D2p/4;
    A1t := Pi*D1t*D1t/4;
    A2t := Pi*D2t*D2t/4;
    A1a := Pi*D1a*D1a/4;
    A2a := Pi*D2a*D2a/4;
    A_ele := W*D + (D_ele/2)*(D_ele/2)*(theta - sin(theta));
```

```
p := 2*(Pi-theta)*D_ele + 2*W;
Dh_ele:= 4*A_ele/p;

Kcon1 := 0.5*(1-(D1t/D1p)*(D1t/D1p));
Kcon2 := 0.5*(1-(D1a/D1t)*(D1a/D1t));
Kcon3 := 0.5*(1-(D2a/Dh_ele)*(D2a/Dh_ele));
Kexp1 := sqr(1-(D1a/Dh_ele)*(D1a/Dh_ele));
Kexp2 := sqr(1-(D2a/D2t)*(D2a/D2t));
Kexp3 := sqr(1-(D2t/D2p)*(D1t/D1p));

Writeln(outfile,'Hydralic diameter of channel ',(Dh_ele/0.0254):0:3,' in');
Writeln(outfile,'Distance between electrodes ',(D/0.0254):0:3,' in');
Writeln(outfile,'Active length ',(L_ele/0.0254):0:3,' in');
Writeln(outfile,'Electrode width ',(W/0.0254):0:3,' in');
Writeln(outfile,'Current = 0.5*Amp/cm^2 ',(W*L_ele*5000):0:3,' Amps');
Writeln(outfile,'Magnetic field strength ',B:0:3,' Tesla');
Writeln(outfile,'Eta for the test section ',(eta1*100):0:2,'%');
Writeln(outfile,'Eta for the acrylic      ',(eta2*100):0:2,'%');
Writeln(outfile,'Eta for the Tygon        ',(eta3*100):0:2,'%');
Writeln(outfile,'Eta for the PVC          ',(eta4*100):0:2,'%');
Writeln(outfile);
Writeln('Hydralic diameter of channel ',(Dh_ele/0.0254):0:3,' in');
Writeln('Distance between electrodes ',(D/0.0254):0:3,' in');
Writeln('Active length ',(L_ele/0.0254):0:3,' in');
Writeln('Electrode width ',(W/0.0254):0:3,' in');
Writeln('Current = 0.5*Amp/cm^2 ',(W*L_ele*5000):0:3,' Amps');
Writeln('Magnetic field strength ',B:0:3,' Tesla');
Writeln('Eta for the test section ',(eta1*100):0:2,'%');
Writeln('Eta for the acrylic      ',(eta2*100):0:2,'%');
Writeln('Eta for the Tygon        ',(eta3*100):0:2,'%');
Writeln('Eta for the PVC          ',(eta4*100):0:2,'%');
Writeln;
write('Volts   Vel(m/sec)  Flow(GPM)');
writeln('   Eff(%)     Current(A)    alpha');
writeln;
write(outfile,'Volts   Vel(m/sec)  Flow(GPM)');
writeln(outfile,'   Eff(%)     Current(A)    alpha');
writeln(outfile);
For count := 1 to 21 do
  Begin
    V := 11 + 3*(count-1);
    GetU(U,I,eta,0,50,V);
    M_H := I*C_H;
    M_Cl := I*eta1*C_Cl;
    Chi_Ts := (M_H+M_Cl)/(A_ele*rho*U);
    Rt:= Rf(Chi_TS)*(f(U)*L_ele/Dh_ele)*U*U/2 + dpa(U,Chi_Ts);
    Rt := Rt/(f(U)*L_ele*U*U/(2*Dh_ele));
    gpm := A_ele*U*1.585e+4;
    Re := U*Dh_ele/nu;
    writeln(V:4:1,U:12:6,gpm:13:6,eta*100:11:6,I:12:6,alpha(Chi_TS):10:5);
    writeln(outfile,V:4:1,U:12:6,gpm:13:6,eta*100:11:6,I:12:6,alpha(Chi_TS)
  end;
Write('Hit return to continue');
readln;
close(outfile);
{clrscr;}
Write('Would you like to have the results printed : ');
readln(letter);
if letter in ['Y','y'] then
begin
```

```
      Swapvectors;
      Exec(GetEnv('COMSPEC'),'/C'+ command);
      Swapvectors;
    end;
    write('Would you like to try another set-up : ');
    readln(letter);
    flag := NOT (letter in ['Y','y']);
  until flag
end.   {Main Program}
```

Appendix B

COMPUTER CODE USED TO PREDICT PERFORMANCE OF A HELICAL THRUSTER

```
Program Helix;
{$R+}
{$D+}
{$S-}
{$M 8192,0,0}
uses crt,Dos;

{All units will be in SI units}

Const
  Sigma = 5;
  nu    = 1.181e-6;
  rho   = 1025;
  tol   = 0.001;
  kin   = 0.5;
  kout  = 1;
  vf    = 1/rho;
  C_Cl  = 3.6809E-7;
  C_H   = 1.0464E-8;
{  C_Cl = 0;
  C_H = 0;}
  rho_H = 0.0837;
  rho_Cl = 2.9944;
  Vo  = 2.25;

Var
  W,                    {Width of the electrodes}
  H,                    {Height of test section}
  D,                    {Distance between electrodes}
  L_ele,L_bend,         {Length of the electrodes}
  R0,                   {Radius of centerline}
  A_ele,                {Cross-Sectional flow area of test section}
  p,                    {Wetted perimeter of test section}
  Dh_ele,               {Hydraylic Diameter of test section}
  L1pa,                 {Length of vertical PVC   on bottom half of loop}
  L1pb,                 {Length of horizontal PVC "    "     "   "    " }
  D1p,L1p,A1p,          {Inner Diameter, Length, Area of lower PVC pipe}
  D2p,L2p,A2p,          {  "      "        "      "   "  upper  "   "  }
  D1t,L1t,A1t,          {  "      "        "      "   "  lower tygon tubing}
  D2t,L2t,A2t,          {  "      "        "      "   "  upper   "      "  }
  D1a,L1a,A1a,          {  "      "        "      "   "  lower acrylic tubing}
  D2a,L2a,A2a,          {  "      "        "      "   "  upper    "      "   }
  rd,                   {Ratio of Radius of Curvature to Hydraulic Diameter}
  R,                    {Electrical Resistance which the electrodes see}
  U,                    {Water Velocity through the test section}
  Re,                   {Reynolds # of the flow in the test section}
  I,                    {Electrical current through the test section}
  I_fix,                {Desired current for the current mode}
  V,                    {Voltage difference between the electrodes}
  eta,                  {Induction efficency for the test section}
  gpm,                  {Flow rate through the test section in GPM }
  B,                    {Magnetic Field Strength}
  Rt,                   {Total two phase multiplier}
  M_H,                  {Mass production rate of Hydrogen}
  M_Cl,                 {  "       "       "   "  Chlorine}
  Chi,                  {Mass percentage of Gas at any point in the loop,
                         Quality}
  eta1                  {% of undissolved Cl in test section},
  eta2,                 {" "      "        " "  return acrylic}
  eta3,                 {" "      "        " "    "    tygon}
```

```
  eta4,                 {" "      "        " "    "    PVC}
  K1,                   {from 2 in PVC to  2 in TYGON}
  K2,                   {from 2 in Tygon to 1.75 in Acry}
  K3,                   {from 1.75 Acry to test section}
  K4,                   {from test sectio to 1 in Acryl}
  K5,                   {from 1.75 Acryl to 2 Tygon}
  K6,                   {from 2 Tygon to 2 PVC}
  dcathode,             {inner diameter of cathode}
  danode,               {outer diameter of anode}
  totheight,            {height of helix}
  finwidth,             {width of helix fins}
  mid_height            {Height of the helix midplanewrt to magnet midplane}  : R

  count,n,nmax,nmin       : Integer;
  outfile                 : text;
  outname                 : string[35];
  temp                    : string[20];
  command                 : string[50];
  letter                  : char;
  flag,modvolt            : boolean;


{*************************************************************************}
{*************************************************************************}
{*************************************************************************}

Function vg:real;

  {This function calculates the specific volume of the 'equivelent gas' }

Var
  vg_temp : real;

Begin
  vg_temp:= ((1/rho_h) + (1/rho_Cl))/(2);
  vg := vg_temp;
End;




{*************************************************************************}
{*************************************************************************}
{*************************************************************************}

Function alpha(X : real):real;

  {This function calculates the void fraction given a quality}

VAR
 al_temp : real;

Begin

  If (X<=0) then
    al_temp := 0
  else
    al_temp := 1/(1+((1-X)/X)*(vf/vg));
  alpha := al_temp;
End;
```

```
{*************************************************************************}
{*************************************************************************}
{*************************************************************************}

Procedure GetI(Var I1,Chi_i: real ;B_loop,U_TS,V_ele,Chi_st :real);

  Var
    I2,I_large,Ismall   : Real;
    difference : real;
    M_H, M_CL_init,Chi,mdot : real;
    mg : real;

Begin
   I_large := 500;
   Ismall := 0;
   Repeat
     I1 := (I_large+Ismall)/2;
     mdot := A_ele*rho*U_TS;
     M_H := C_H*I1;
     M_CL_init := I1*C_Cl;
     M_CL := eta1*M_Cl_init;
     mg := M_H + M_Cl;
     Chi_i:= Chi_st + mg/(mdot*2);
     R := D/(W*2*Pi*R0*sigma*(1-alpha(Chi_i)));
     I2 := (V_ele-Vo-B_loop*U_TS*D);
     I2 := I2/R;
     difference := (I1 - I2)/I1;
     If (difference <0) then
       Begin
         I_large:= I2;
         Ismall := I1;
       End
     Else
       begin
         Ismall := I2;
         I_large := I1;
       end;
  until (Abs(difference)<tol);
    Chi_i := Chi_i + mg/(mdot*2);
End;



{*************************************************************************}
{*************************************************************************}
{*************************************************************************}

Function dpa(U,X : real):real;

          {This function calculates the acceleration pressure drop}

VAR
  G,              {Mass flux}
  dpa_temp,
  temp1,temp2 :real;

Begin
  G := rho*U;
  If (X<=0) then
```

```
    dpa_temp := 0
  else
    Begin
      temp1 := vf*((sqr(1-X))/(1-alpha(X)) - 1);
      temp2 := vg*(X*X)/alpha(X);
      dpa_temp := (G*G)*(temp1 + temp2);
    End;
  dpa := dpa_temp;
End;

{*****************************************************************************}
{*****************************************************************************}
{*****************************************************************************}


Function Rf(X:real):real;

  {This function calculates the 2 phase friction multiplier}

VAR
  Rf_temp,
  beta : real;

Begin
  beta := 1/(1-alpha(X));
  Rf_temp := (1/3)*(1+ beta + beta*beta);
  Rf := Rf_temp;
End;

{*****************************************************************************}
{*****************************************************************************}
{*****************************************************************************}


Function f(Rey:real):real;

{This function calulates the friction factor}

VAR
  f_temp : real;

Begin
{  writeln(ln(Rey));}
  if (Rey <= 2300) then f_temp:= 64/Rey
    else if (Rey <= 2e4) then f_temp := exp(ln(0.316) - 0.25*ln(Rey))
      else f_temp:=exp(ln(0.184)-0.2*ln(Rey));
  f:=f_temp;
End;


{*****************************************************************************}
{*****************************************************************************}
{*****************************************************************************}


Function dp1ph(U,Di,L:Real):Real;

{This function calculates the 1 phase frictional pressure drop}

Var
```

```
  Re,
  Temp_dp : Real;


Begin
   Re := U*Di/nu;
   temp_dp := f(Re)*(L/Di)*rho*U*U/2;
   dplph := temp_dp;
End;

{*************************************************************************}
{*************************************************************************}
{*************************************************************************}

Function K(A1,A2 : real):real;

Var
  beta, K_temp    : real;

Begin
  beta := A1/A2;
  If (beta < 1) then
    K_temp := sqr(1 - beta)
  Else
    Begin
      beta := A2/A1;
      K_temp := 0.5*(1- beta*beta);
    End;
  K := K_temp;
End;



{*************************************************************************}
{*************************************************************************}
{*************************************************************************}


Function Dpk(K,U1,A1,A2 : real):real;

Var
  beta, dp,U    : real;

Begin
  beta := A1/A2;
  If (beta < 1) then
    U := U1
  Else
    U := U1*beta;
  dp := K*U*U*rho/2;
  Dpk := dp;
End;



{*************************************************************************}
{*************************************************************************}
{*************************************************************************}
```

```
Procedure GetU(Var Uin, Iu, etau : Real ; small,large,Vu : real);

{This procedure does all of the iterations to find the correct velocity}

  Var
    loop : integer;
    dpf_ele,dpf1a,dpf2a,
    dpf1p,dpf2p,dpf1t,dpf2t,
    dpf,dpfa,dpfp,dpft,
    dpend1,dpend2,dpend,
    prise,diff,
    dpk1,dpk2,dpk3,dpk4,dpk5,dpk6,
    dpec,                          {expansion and contraction}
    M_H,mdot_tot,
    M_Cl,M_Cl_init,Chi,Chi_1,
    U1p,U2p,U1a,U2a,U1t,U2t,
    B_loop,x                              : Real;
    ch      : char;
    I_Loop,prise_1 : array[1..15] of real;

Begin

{ This part of the procedure makes a new a guess at the velocity,
and uses the geometry, to calculate the other parameters.}

{  writeln('new');}
  Uin :=  (small+large)/2;

{  writeln('U : ',Uin:0:4);}
  mdot_tot := Uin*A_ele*rho;
  prise:=0;
  Iu:=0;
  Chi := 0;
  for loop:=1 to n do

      {Note this will distribute the void fraction according to how much
       Current passed downstream of each loop, for the purpose of calculating
       the system current, However the void is evenly smeared thru the test
       section for the dp calculations}

    begin
      x:=((W+finwidth)*(loop-1)+W/2-totheight/2+mid_height)/0.0254;
      B_loop:=B*(1.097+abs(x)*0.0184-0.0232*sqr(x)+0.00125*abs(x*x*x));
      GetI(I_loop[loop],Chi_1,B_loop,Uin,Vu,Chi);
      Iu:=Iu+I_loop[loop];
{      writeln(Chi:6,' ',Chi_1:6,' ',Iu:0:5);  }


      Chi := Chi + Chi_1;

      prise_1[loop]:=I_loop[loop]*B_loop*D/A_ele;
      prise:=prise+prise_1[loop];
    end;

  M_H  := C_H*Iu;
  M_Cl_init := Iu*C_Cl;
  M_CL := etal*M_Cl_init;
  Chi := (M_H+M_Cl)/(mdot_tot*2);

  {This part of the procedure calculates the frictional, and two phase
```

```
acceleration pressure drops for the loop.)

dpf_ele := Rf(Chi)*dp1ph(Uin,Dh_ele,L_ele/0.9+60*Dh_ele + L_bend);
dpf_ele := dpf_ele + dpa(Uin,Chi);


U1p :=(A_ele/A1p)*Uin;
dpf1p  := dp1ph(U1p,D1p,L1p);
U2p := (A_ele/A2p)*Uin;
M_Cl := eta2*M_Cl_init;
Chi := (M_H+M_Cl)/(mdot_tot);
dpf2p := Rf(Chi)*dp1ph(U2p,D2p,L2p);
dpfp := dpf1p + dpf2p;

U1t := (A_ele/A1t)*Uin;
dpf1t  := dp1ph(U1t,D1t,L1t);
U2t := (A_ele/A2t)*Uin;
M_Cl := eta3*M_Cl_init;
Chi := (M_H+M_Cl)/(mdot_tot);
dpf2t := Rf(Chi)*dp1ph(U2t,D2t,L2t);
dpft := dpf1t + dpf2t;

U1a := (A_ele/A1a)*Uin;
dpf1a  := dp1ph(U1a,D1a,L1a) ;
U2a := (A_ele/A2a)*Uin;
M_Cl := eta4*M_Cl_init;
Chi := (M_H+M_Cl)/(mdot_tot);
dpf2a := Rf(Chi)*dp1ph(U2a,D2a,L2a);
dpfa := dpf1a + dpf2a;

dpf  := dpf_ele + dpfp + dpft + dpfa;
{  write('Test Section : ',dpf_ele:0:1,' PVC : ',dpfp:0:1);
writeln(' Tygon : ',dpft:0:1,' Acrylic : ',dpfa:0:1);
writeln('Total Friction : ',dpf:0:1);                          }

{This calculates the pressure drop associates with the tank entrance and
exit.}

dpend1 := kin*rho*U1p*U1p/2;
dpend2 := kout*rho*U2p*U2p/2;
dpend  := dpend1+dpend2;
{  write('Tank outlet: ',dpend1:0:1,' Tank inlet :  ',dpend2:0:1);
writeln(' Total Tank : ',dpend:0:1);                           }

{The next set of calculations calculates the expansion and contraction
losses throughout the loop.  The format is generic, the code will determine
whether it is a contraction or expansion based on the the areas.}

dpk1 := dpk(K1,U1p,A1p,A1t);
dpk2 := dpk(K2,U1t,A1t,A1a);
dpk3 := dpk(K3,U1a,A1a,A_ele);
dpk4 := dpk(K4,Uin,A_ele,A2a);
dpk5 := dpk(K5,U2a,A2a,A2t);
dpk6 := dpk(K6,U2t,A2t,A2p);
{  write('Form losses 1-6 : ',dpk1:0:1,' ',dpk2:0:1,' ',dpk3:0:1,' ');
writeln(dpk4:0:1,' ',dpk5:0:1,' ',dpk6:1:1);                   }
dpec := dpk1 + dpk2 + dpk3 + dpk4 + dpk5 + dpk6;
{  writeln('Total form losses : ',dpec:0:1);                   }
```

```
  {This is the pressure rise associated with the thruster}

{  writeln('Thruster Pressure rise : ',prise:0:1);              }

  {This determines whether the pressure rise in the thruster is larger than
  the loop pressure drop.  If this is the case a larger velocity is used,
  if the loop pressure drop is larger a smaller velocity is used as the next
  guess.}

  etau:=prise*A_ele*Uin/(Vu*Iu);
  diff  := (prise - dpf - dpend - dpec)/(prise);
  if (abs(diff)>tol) and (diff<0) then
  GetU(Uin,Iu,etau,small,Uin,Vu)
    else if (abs(diff)>tol) and (diff>0) then  GetU(Uin,Iu,etau,Uin,large,Vu)
      else
end;

{*****************************************************************************}
{*****************************************************************************}
{*****************************************************************************}


Procedure GetUV(Var Uin, Vu, etau : Real ; small,large,Ireq : real;Var Iu:real);

{This procedure does all of the iterations to find the correct velocity}


  Var
    loop : integer;
    dpf_ele,dpf1a,dpf2a,
    dpf1p,dpf2p,dpf1t,dpf2t,
    dpf,dpfa,dpfp,dpft,
    dpend1,dpend2,dpend,
    prise,diff,diff_I,
    dpk1,dpk2,dpk3,dpk4,dpk5,dpk6,
    dpec,                        {expansion and contraction}
    M_H,mdot_tot,
    M_C1,M_C1_init,Chi,Chi_1,
    U1p,U2p,U1a,U2a,U1t,U2t,x,B_loop      : Real;
    Vsmall,vlarge                        : Real;
    I_loop,prise_1 : array[1..15] of real;
    ch      : char;

Begin

{ This part of the procedure makes a new a guess at the velocity,
and uses the geometry, to caclulate the other parameters.}

  Uin :=  (small+large)/2;

{ writeln('new');                                              }
{  writeln('U : ',Uin:0:4);                                    }


  mdot_tot := Uin*A_ele*rho;
  etau := (Uin*B*D)/Vu;

  {This part of the procedure calculates the frictional, and two phase
  acceleration pressure drops for the loop.}
```

```
Vlarge:= 500;
Vsmall := 0;

repeat
  Chi:=0;
  prise:=0;
  Iu:=0;
  {If (abs((Vu - Vlarge)/Vlarge) <  tol) then
   Begin
     writeln(Vlarge:0:3,' ',vsmall:0:3,' ',Vu:0:3);
     writeln('here');
     Vsmall := Vlarge;
     Vlarge := 2*Vlarge;

   end; }
  Vu := (Vlarge + Vsmall)/2;
  for loop:=1 to n do
    begin
      x:=((W+finwidth)*(loop-1)+W/2-totheight/2 + mid_height)/0.0254;
      B_loop:=B*(1.097+abs(x)*0.0184-0.0232*sqr(x)+0.00125*abs(x*x*x));

      {Note this will distribute the void fraction according to how much
       Current passed downstream of each loop, for the purpose of calculating
       the system current, However the void is evenly smeared thru the test
       section for the dp calculations}

      GetI(I_loop[loop],Chi_1,B_loop,Uin,Vu,Chi);
      Iu:=Iu+I_loop[loop];
      Chi := Chi + Chi_1;
      prise_1[loop]:=I_loop[loop]*B_loop*D/A_ele;
      prise:=prise+prise_1[loop];
    end;
  diff_I := (Iu - Ireq)/(Ireq);
  if (diff_I<0) then
    Vsmall := Vu
  else
    Vlarge := Vu;
until (abs(diff_I) < tol);

M_H  := C_H*Iu;
M_Cl_init := Iu*C_Cl;
M_CL := eta1*M_Cl_init;
Chi := (M_H+M_Cl)/(mdot_tot*2);


dpf_ele := Rf(Chi)*dp1ph(Uin,Dh_ele,L_ele/0.9+60*Dh_ele + L_bend);
dpf_ele := dpf_ele + dpa(Uin,Chi);


U1p :=(A_ele/A1p)*Uin;
dpf1p  := dp1ph(U1p,D1p,L1p);
U2p := (A_ele/A2p)*Uin;
M_Cl := eta2*M_Cl_init;
Chi := (M_H+M_Cl)/(mdot_tot);
dpf2p := Rf(Chi)*dp1ph(U2p,D2p,L2p);
dpfp := dpf1p + dpf2p;

U1t := (A_ele/A1t)*Uin;
dpf1t  := dp1ph(U1t,D1t,L1t);
U2t := (A_ele/A2t)*Uin;
```

```
  M_Cl := eta3*M_Cl_init;
  Chi := (M_H+M_Cl)/(mdot_tot);
  dpf2t := Rf(Chi)*dp1ph(U2t,D2t,L2t);
  dpft := dpf1t + dpf2t;

  U1a := (A_ele/A1a)*Uin;
  dpf1a  := dp1ph(U1a,D1a,L1a) ;
  U2a := (A_ele/A2a)*Uin;
  M_Cl := eta4*M_Cl_init;
  Chi := (M_H+M_Cl)/(mdot_tot);
  dpf2a := Rf(Chi)*dp1ph(U2a,D2a,L2a);
  dpfa := dpf1a + dpf2a;

  dpf  := dpf_ele + dpfp + dpft + dpfa;
{ write('Test Section : ',dpf_ele:0:1,' PVC : ',dpfp:0:1);
  writeln(' Tygon : ',dpft:0:1,' Acrylic : ',dpfa:0:1);
  writeln('Total Friction : ',dpf:0:1);                          }

  {This calculates the pressure drop associates with the tank entrance and
  exit.}

  dpend1 := kin*rho*U1p*U1p/2;
  dpend2 := kout*rho*U2p*U2p/2;
  dpend  := dpend1+dpend2;
{ write('Tank outlet: ',dpend1:0:1,' Tank inlet :  ',dpend2:0:1);
  writeln(' Total Tank : ',dpend:0:1);                           }

  {The next set of calculations calculates the expansion and contraction
  losses throughout the loop.  The format is generic, the code will determine
  whether it is a contraction or expansion based on the the areas.}

  dpk1 := dpk(K1,U1p,A1p,A1t);
  dpk2 := dpk(K2,U1t,A1t,A1a);
  dpk3 := dpk(K3,U1a,A1a,A_ele);
  dpk4 := dpk(K4,Uin,A_ele,A2a);
  dpk5 := dpk(K5,U2a,A2a,A2t);
  dpk6 := dpk(K6,U2t,A2t,A2p);
{ write('Form losses 1-6 : ',dpk1:0:1,' ',dpk2:0:1,' ',dpk3:0:1,' ');
  writeln(dpk4:0:1,' ',dpk5:0:1,' ',dpk6:1:1);                   }
  dpec := dpk1 + dpk2 + dpk3 + dpk4 + dpk5 + dpk6;
{ writeln('Total form losses : ',dpec:0:1);                      }


  {This is the pressure rise associated with the thruster}

  prise  := (Iu*B*D)/A_ele;
{ writeln('Thruster Pressure rise : ',prise:0:1);                }

  {This determines whether the pressure rise in the thruster is larger than
  the loop pressure drop.  If this is the case a larger velocity is used,
  if the loop pressure drop is larger a smaller velocity is used as the next
  guess.}

  diff  := (prise - dpf - dpend - dpec)/(prise);
  if (abs(diff)>tol) and (diff<0) then
    GetUV(Uin,Vu,etau,small1,Uin,Ireq,Iu)
  else if (abs(diff)>tol) and (diff>0) then
    GetUV(Uin,Vu,etau,Uin,large,Ireq,Iu)
      else
end;
```

```
{*****************************************************************************}
{*****************************************************************************}
{*****************************************************************************}

Begin  {Main Program}
  repeat
    clrscr;
    write('filename = ');
    readln(temp);
    outname :=  'c:\turbo\helix\' + temp +'.dat';
    assign (outfile,outname);
    command := 'print '+ outname;
    rewrite (outfile);
    B := 7.5;
    write('Min Number of Loops = ');
    readln(nmin);
    write('Max Number of Loops = ');
    readln(nmax);
    Write('Cathode Diameter = ');
    Readln(dcathode);
    dcathode := dcathode*0.0254;
    write('Anode Diameter = ');
    readln(danode);
    danode := danode*0.0254;
    write('Finwidth = ');
    readln(finwidth);
    finwidth := finwidth*0.0254;
    write('Helix length = ');
    readln(totheight);
    totheight := totheight*0.0254;
    write('Height of helix midplane wrt magnet midplane = ');
    readln(mid_height);
    mid_height := mid_height*0.0254;
    repeat
       write('Would like a Current(C) or Voltage(V) : ');
       readln(letter);
    until letter in ['C','c','v','V'];

    modvolt := letter in ['v','V'];
    if modvolt then
      begin
          write('Voltage = ');
          readln(V);
       end
    else
      begin
        write('Current = ');
```

```
    readln(I_fix);
  end;
clrscr;
for n := nmin to nmax do
  begin
    R0 := (dcathode+danode)/4;
    D := (dcathode-danode)/2;
    W := (totheight-finwidth*(n-1))/n;
    H := W;

    D1p := 2.067*0.0254;
    D2p := 2.067*0.0254;
    D1t := 2*0.0254;
    D2t := 2*0.0254;
    D1a := 1.75*0.0254;
    D2a := 1.75*0.0254;

    eta1 := 1.00;
    eta2 := 1.00;
    eta3 := 1.00;
    eta4 := 1.00;

    A1p := Pi*D1p*D1p/4;
    A2p := Pi*D2p*D2p/4;
    A1t := Pi*D1t*D1t/4;
    A2t := Pi*D2t*D2t/4;
    A1a := Pi*D1a*D1a/4;
    A2a := Pi*D2a*D2a/4;
    A_ele := H*D;
    p := 2*(H + D);
    Dh_ele:= 4*A_ele/p;
    rd := R0/Dh_ele;

    L1a := 10*0.0254 + 30*D1a;
    L2a := 10*0.0254;
    L1pa := (22*0.0254);
    L1pb := (75*0.0254);
    L1p := L1pa + L1pb + 86*D1p;
    L2p := (53*0.0254) + 3*D2p;
    L1t :=  24*0.0254;
    L2t := 33*0.0254 + 30*D2t;
    L_ele := R0*2*Pi*n;

    If (rd = 1) then
      L_bend := 20
    Else
    IF (rd < 1.5) then
      L_bend := 20 - (rd - 1)*12
    Else
    If (rd < 2) then
      L_bend := 14 - (rd - 1.5)*4
    Else
    If (rd < 3) then
      L_bend := 12
    Else
    If (rd <  4) then
      L_bend := 12 + (rd - 3)*2
    Else
    If (rd < 6) then
      L_bend := 14 + (rd-4)*1.5
```

```
        Else
          L_bend := 25;

        L_bend := (n*4-1)*(0.25*Pi*rd + 0.5*L_bend) + L_bend;
        L_bend:= L_bend*Dh_ele;


        K1 := K(A1p,A1t);
        K2 := K(A1t,A1a);
        K3 := K(A2a,A_ele);
        K4 := K(A_ele,A2a);
        K5 := K(A2a,A2t);
        K6 := K(A2t,A2p);

        If modvolt then
          GetU(U,I,eta,0,V*2,V)
        else
          GetUV(U,V,eta,0,I_fix/10,I_fix,I);

        gpm := A_ele*U*1.585e+4;
        Write('N = ',n,'              D = ',(D/0.0254):0:3);
        Writeln('       W = ',W/0.0254:0:3,'    Fin Width = ',finwidth/0.0254:0:
        write('GPM = ',gpm:6:3,'     eta = ',eta*100:0:3,'     I = ',I:0:1);
        writeln('     V = ',V:0:1);
        writeln;
        writeln(outfile,n:3,gpm:12:6,eta*100:12:6,I:12:6,(d/0.0254):12:3);
        {Write('Hit return to continue');
              readln;}
      end;
    close(outfile);
    write('Would you like to try another set-up : ');
    readln(letter);
    flag := (letter in ['N','n']);
  until flag
end.   {Main Program}
```